NORTH CAROLINA A&T STATE UNIVERSITY
Greensboro, NC 27411
School of Engineering

Final Report

"FRACTURE PREDICTION IN BRITTLE MATERIALS"

Contract No. N00019-78-C-0520

May 29, 1981

William J. Craft
Principal Investigator
Assistant Dean and Professor
Mechanical Engineering
(919) 379-7549

George J. Filatovs
Co-Investigator
Associate Professor
Mechanical Engineering
(919) 379-7620

Unclassified

SECURITY CLASSIFICATION OF THIS PAGE (When Data Entered)

REPORT DOCUMENTATION PAGE

READ INSTRUCTIONS BEFORE COMPLETING FORM

1. REPORT NUMBER 34020122	2. GOVT ACCESSION NO. AD-A112 452
3. RECIPIENT'S CATALOG NUMBER	
4. TITLE (and Subtitle) Fracture Prediction in Brittle Materials	5. TYPE OF REPORT & PERIOD COVERED Final
	6. PERFORMING ORG. REPORT NUMBER 34020122
7. AUTHOR(s) William J. Craft, George J. Filatovs	8. CONTRACT OR GRANT NUMBER(s) N00019-78-C-0520
9. PERFORMING ORGANIZATION NAME AND ADDRESS School of Engineering, North Carolina A&T State University, 312 N Dudley Street, Greensboro, NC 27411	10. PROGRAM ELEMENT, PROJECT, TASK AREA & WORK UNIT NUMBERS
11. CONTROLLING OFFICE NAME AND ADDRESS Department of the Navy, Naval Air Systems Command and Air Systems Command Headquarters, Washington, D. C. 20361	12. REPORT DATE May 29, 1981
	13. NUMBER OF PAGES 128
14. MONITORING AGENCY NAME & ADDRESS(if different from Controlling Office)	15. SECURITY CLASS. (of this report) Unclassified
	15a. DECLASSIFICATION/DOWNGRADING SCHEDULE

16. DISTRIBUTION STATEMENT (of this Report)

Approved for Public Release - Distribution Unlimited

17. DISTRIBUTION STATEMENT (of the abstract entered in Block 20, if different from Report)

18. SUPPLEMENTARY NOTES

19. KEY WORDS (Continue on reverse side if necessary and identify by block number)

Ceramics, Brittle Materials, Alumina, Mullite (MV33), Weibull Parameters, Ceramic Tubes, 4-Point Bending, Fracture Mechanics

20. ABSTRACT (Continue on reverse side if necessary and identify by block number)

The use of ceramics in scientific and industrial applications is limited by their relatively poor mechanical properties, brittleness and variability in strength. Design with brittle materials requires an entirely new concept from that with ductile materials. One must think in terms of probability rather than virtual certainty.

DD FORM 1 JAN 73 1473 EDITION OF 1 NOV 65 IS OBSOLETE

S/N 0102-LF-014-6601

Unclassified

SECURITY CLASSIFICATION OF THIS PAGE (When Data Entered)

(Question 20 continued)

Statistical flaw theory based on the "weakest-link" hypothesis has been applied to problems of fracture and failure of brittle materials under test loads. One such theory, the Weibull distribution, which is probably the most widely applied, addresses the statistical variation of strength and the size effect due to flaws, because in a variety of conditions both its mathematical formulation and the estimation of the Weibull parameters from experiments are simple. Many techniques exist to determine the Weibull parameters from the series of data obtained from experimental tests.

The Log-Log Method is developed for the three-parameter family distribution of both the uniaxial constant stress field and pure bending field in a rectangular section bar. This provides for redefining the dynamic weights assigned to data points iteratively to emphasize the leading distribution data or to de-emphasize errant points. This method is compared with those obtained from the Moment Generating Method and the Newton-Raphson iteration method for the case of uniaxial constant stress fields.

The Weibull distribution expressions have been developed for the pure bending and torsion stress states for the fracture of hollow alumina tubes. Such tests are relatively inexpensive and provide useful data reliably but no closed-form solution exists for the probability formulations. An iteration method based on the least-square minimization of residual errors in the test results is used to determine the Weibull parameters.

A simple theory which bypasses the assumptions of independence under multiaxial stress states and defines all Weibull parameters as data points about the $\hat{n} = (1,1,1)\sqrt{3}$ vector in principal stress space is developed. This allows an extrapolation of biaxially determined data to the general three-dimensional stress state when an axis of symmetry exists. In this case, from a table of experimentally determined Weibull parameters based on biaxial data, a single independent variable determines the probability of failure of the material in an arbitrary stress field.

ABSTRACT

The use of ceramics in scientific and industrial applications is limited by their relatively poor mechanical properties, brittleness and variability in strength. Design with brittle materials requires an entirely new concept from that with ductile materials. One must think in terms of probability rather than virtual certainty.

Statistical flaw theory based on the 'weakest-link' hypothesis has been applied to problems of fracture and failure of brittle materials under test loads. One such theory, the Weibull distribution, which is probably the most widely applied, addresses the statistical variation of strength and the size effect due to flaws, because in a variety of conditions both its mathematical formulation and the estimation of the Weibull parameters from experiments are simple. Many techniques exist to determine the Weibull parameters from the series of data obtained from experimental tests.

The Log-Log Method is developed for the three-parameter family distribution of both the uniaxial constant stress field and pure bending field in a rectangular section bar. This provides for redefining the dynamic weights assigned to data points iteratively to emphasize the leading distribution data or to de-emphasize errant points. This method is compared with those obtained from the Moment Generating Method and the Newton-Raphson iteration method for the case of uniaxial constant stress fields.

The Weibull distribution expressions have been developed for the pure bending and torsion stress states for the fracture of hollow alumina

tubes. Such tests are relatively inexpensive and provide useful data reliably but no closed-form solution exists for the probability formulations. An iteration method based on the least-square minimization of residual errors in the test results is used to determine the Weibull parameters.

A simple theory which bypasses the assumptions of independence under multiaxial stress states and defines all Weibull parameters as data points about the $\hat{n} = (1,1,1)\sqrt{3}$ vector in principal stress space is developed. This allows an extrapolation of biaxially determined data to the general three-dimensional stress state when an axis of symmetry exists. In this case, from a table of experimentally determined Weibull parameters based on biaxial data, a single independent variable determines the probability of failure of the material in an arbitrary stress field.

ACKNOWLEDGEMENT

This report and research paper published to date were made possible through NAVAL AIR SYSTEMS COMMAND Contract No. N00019-78-C-0520. The investigators are grateful for this support and hope that this work will provide more economical testing procedures of increased accuracy for Weibull materials used in structural applications.

TABLE OF CONTENTS

LIST OF TABLES

LIST OF FIGURES

Figure		Page
4.15	Multiple Compression Compound Fracture of Alumina Specimen A11	58
4.16	Two-Section Fracture With a Compression Axial Split in Alumina Specimen A17	59
4.17	Mullite Bend Specimen M19 Multiple Fracture	59
4.18	Mullite Bend Specimen M1 Multiple Fracture	60
4.19	Mullite Bend Specimen M20 Multiple Fracture	60
B.1	Selection of Three Data Points	74
C.1	Probability Distribution	79
C.2	Cumulative Frequency Distribution of Table C.1 Data	80
C.3	Probability of Failure for the Data of Table C.1	81
D.1	The Weibull Distribution for Different Values of m	85

NOMENCLATURE

σ = Fracture Stress

ν = Poisson's ratio

E = Youngs Modulus

σ_{ut} = Ultimate Tensile Stress

σ_{uc} = Ultimate Compressive Stress

V = Volume of Material under stress

V_{un} = Unit Volume of Material under stress

$P(\sigma)$ = Probability density function, p.d.f., for Volume, V

$f(\sigma)$ = Probability density function, p.d.f., for elemental Volumes, v_i

$g(\sigma)$ = Cumulative distribution function, c.d.f., for elemental Volumes, v_i

$F(\sigma)$ = Cumulative distribution function, c.d.f., for Volume, V

$F(\tilde{\sigma})$ = Probability of fracture by Mean Rank or Median Rank Methods, etc.

σ_u = Threshold Stress

m = Weibull Modulus, Shape Parameter

σ_o = Scale Parameter

c = Constant

M = Bending Moment

T = Torque

I = Moment of Inertia

J = Polar Moment of Inertia

L = Length of Specimen

w = Arbitrary weights assigned to data points

ℓn = Natural Logarithm

exp = Exponential Base of Natural Logarithm

CHAPTER I

INTRODUCTION

Ceramics are inorganic non-metallic brittle materials which have been used by mankind for centuries. In ancient times they were used primarily as materials for pottery and artwork because of their unique properties of stability and aesthetic appeal. The survival of pottery over centuries illustrates one of the great advantages which ceramics possess over most materials; their durability. On the other hand, ceramics lacked uniformity and reproducibility. Until three decades or so ago, users of ceramics procurred their material from one source and one particular plant of a supplier in order to maintain uniformity. Ceramic producers were reluctant to change any detail of their processing and manufacturing. The reason was that the complex material systems being used were not sufficiently known at that time to allow the effect of changes to be predicted or understood.

Today, because of the possibility of technological control of the mechanical properties of ceramics and related materials they have become issues of major importance. Now these materials are used in a number of scientific and industrial applications such as turbine blades, prosthetics, ceramic bearings, and the like [1]. The rapid growth in particular, of the electronics industry has demanded the development of many specialized types of ceramic insulators. One of the important reasons why ceramics find such wide application in a wide variety of fields is that these materials exhibit a wide range of desirable properties. For example, properties of individual ceramics include

resistance to heat, oxidation, corrosion, and abrasion; high elastic modulus, high strength, and low density with applications to the nuclear, optical, magnetic, electronic, and other industries. Other applications are much too long to list here in detail, but some examples will serve to illustrate the great diversity and importance of these materials. Special electrical properties form the basis for applications as insulators, piezoelectric transducers, and an ever-increasing family of semiconductor devices. In the past twenty years a great many new types of ceramic insulators have been produced which included alumina, magnesia, beryllia, zirconia and so on. The recent use of barium titanate, when placed between the plates of an electrical capacitor allowed it to store several thousand times the amount of charge that could be stored by the same capacitor if air were used instead. This had lead to the production of a series of related materials called ferroelectrics which have helped make electronic equipment lighter and smaller. Magnetic ceramics include cores for computer memories and permanent magnets for electric motors.

Special chemical and thermal properties are exploited in furnaces and crucibles which are essential to the refining, alloying, and casting of metals. 'Thermistor' is a special kind of ceramic whose electrical resistivity varies with changing temperature and is used as a temperture sensing and control element in automated manufacturing processes. Thermoelectric properties are important in developing solar cells supplying energy for satellites [2]. The high elastic moduli and hardness of certain ceramics make them suitable for special applications requiring mechanical stablity such as gyroscope mounts and wear

surfaces while the extremely low thermal expansion achievable is appropriate to telescope mirrors and to applications involving thermal shock.

The advent of the missile and the space age has produced exceptional demands for materials which will stand extremes in temperature and in other environmental conditions. Ceramic materials such as carbides and graphites are being used in some rocket nozzles where temperatures in excess of 5000°F are developed. The high speed of sound in certain ceramics has led to their successful use in armor, and low damping characteristic of many ceramics makes them useful as delay lines.

In our atomic age, as atomic energy becomes commercially competitive with other sources of energy, more efficient nuclear reactors are being produced requiring extreme operating temperatures and absolute mechanical integrity for thousands of hours. The thermal stability of certain nuclear ceramics has led to their adoption as fuel elements for power reactors and in many cases, several functions must be present simultaneously. Because of their extreme hardness, especially at high temperatures, ceramics are widely used for cutting and grinding tools in industry [2]. However, their use as an abrasive has been limited by the fact that they generally do not form sharp cutting edges as they wear away (friability). Many different optical properties of ceramic products are of concern in different applications. Perhaps the most important are those optical glasses and crystals used as windows, lenses, prisms, filters or in other ways requiring useful optical properties as the primary function of the material.

In citing these burgeoning uses, however, one must face the historic problem of brittleness and unpredictability in mechanical properties of

ceramics. These characteristics still remain dictating the need to develop more sophisticated mechanisms to promote general design with ceramics. Further a polycrystalline ceramic is usually made up of one or more phases, grains and pores of various sizes and distributions and impurities inside the grains and in the grain boundaries. All of these, in addition to processing methods, influence the properties of ceramics [3]. For these reasons, it is not a straightforward task to formulate design procedures.

Another obstacle to the wider utilization of ceramics is that they fail with 'glass-like' brittle fracture. They do not normally exhibit appreciable plastic deformation and their impact resistance is low [4]. This is one of the important reasons that the application of ceramics in an engineering sense is limited by these relatively poor mechanical properties, and presently the only generally accepted way of coping with this problem is by gross overdesign and limiting ceramics to areas where structural functions have secondary consideration [5].

If ones attention is focused on the simplest case of the failure of ceramics, then the effects of multiaxial stresses, temperature, strain rate, and time dependency are neglected; and only σ, the uniaxial stress, is considered. A group of properties -- fracture toughness, effective surface energy and work of fracture -- is also important. In some cases these are related directly to strength. This group gives an indication of whether a flaw will propagate or not. Defining γ_i is an effective surface energy for the initiation of fracture from an inherent flaw of size c, a statement of fracture toughness is:

$$\sigma = \frac{1}{Y}\left(\frac{2E\gamma_i}{c}\right)^{\frac{1}{2}} \qquad (1\text{-}1)$$

where Y is a geometrical constant and E, Young's modulus. $(2E\gamma_i)^{1/2}$ is equal to the stress intensity factor. Also related to γ_i is the work of fracture γ_f, defined as the energy required to generate a unit area of fracture face. In general $\gamma_f > \gamma_i$ but when γ_f is measured in a test involving slow controlled crack growth (rather than a partly catastrophic crack growth) $\gamma_f = \gamma_i$ [6].

From the engineering point of view, ductility is a valuable material property not only because ductile materials can undergo a large plastic deformation long before failure but also because ductility leads to increased contact area where high stresses may occur near boundaries, dissipating stress concentrations. Further, ductile materials such as metal can be made and purchased in standard forms such as sheet, tube, and rod etc., which can be deformed into the required shape and joined to form structures. Brittle materials must in general be used in the shape in which they emerge from the factory. In a more specific engineering sense, brittle materials have the characteristic that they are unable to disperse high local stresses which results in undesirable consequences for design engineers. The very low ductility and strain to failure accompanying brittle materials result in a fundamental distinction between the mechanical strength characteristics of ductile and brittle materials. Material property test results for nominally identical steel specimens such as yield and ultimate strength will seldom differ from specimen to specimen by more than 5%; and a minimum value or the mean value alone is a satisfactory basis for design whereas a particular 'static' strength property test on brittle specimens may show a variation of 100% or more [7], depending on the number and size

of the specimens. It has been reasonably established that this variability is not a result of badly controlled specimen preparation or test procedure but it is an inherent characteristic of brittle materials which do not exhibit plastic deformation under stress [8]. Thus, the average or mean strength value is not an adequate basis for specification for engineering design; the variability must be assessed and taken into account in brittle materials. Designing with brittle materials does not require simply different numerical values for the properties of material but a new concept is required to define the strength, and more important, the designer must think in terms of probability rather than virtual certainty.

One such concept is known as the 'weakest-link' concept and it assumes that fracture of the bulk specimen is determined by the local strength of its weakest volume element. The 'weakest-link' hypothesis states that brittle materials fail when the stress intensity at any one flaw in the material reaches the critical value for crack propagation. If flaws are uniformly distributed throughout the material then the number of flaws present in a specimen is proportional to its volume. This is one reason why large specimens are expected to be weaker than smaller ones [9]. In addition to these variations, the use of brittle materials in structural components introduces two more difficulties to efficient, reliable structural design. They are (1) variability in mechanical properties, including the infrequent but real possibility of low values, particularly in large volumes of material, and (2) the accurate definition of the important lower proba-

bility of fracture part of the probability distribution curve, which is necessary if a reliable prediction of failure probability is to be made for large volumes [10]. Since catastrophic failure is commonly induced in the brittle materials, once the 'fracture' stress has been reached, additional and more information may be needed for the use of such materials in an engineering sense.

The weakest-link concept has been widely used in developing various statistical theories of strength which differ from each other only in the way in which the use of the concept is justified, or in the assumed form of the distribution function of local strength. Its application to a solid volume was first proposed by Weibull [11] who, arrived at a distribution function which, now is being widely used for the statistical interpretation of a variety of test data [12] . This theory, applied to brittle materials, addresses the statistical variation of strength and the size effect due to flaws. By assuming that only tension contributes to fracture (fibers in compression have a zero probability of fracture) , Weibull extended the theory to bending, and to any uniaxial combination of bending and tension. Weibull also extended his theory to failure for polyaxial stress states, although it has been questioned by many authors [13,14].

The effect of a biaxial stress field on the fracture behavior of polycrystalline alumina ceramics was studied by Broutman and Cornish [15]. The various stress states of tension-compression, tension-tension and compression-compression were generated in the walls of thin-walled

cylinders by the use of combinations of internal pressure, external pressure, and axial loading. Their results for the two stress ratios investigated in the tension-tension region indicate that the biaxial tensile strength is less than the uniaxial. The results in the tension-compression quadrant were obtained by a combination of axial compressive loading and internal pressure to produce hoop tension. The experimental results indicated that the tensile strength increased when compressive stress existed in the direction normal to the tensile stress. Weibull's theory did not fit the data well as large amounts of scatter were noted in the results. Broutman, et. al. [16] showed that the experimental data in the tension-compression quadrant followed the Coulomb-Mohr theory approximately;

$$\left(\frac{\sigma_1}{\sigma_{ut}}\right) - \left(\frac{\sigma_2}{\sigma_{ue}}\right) = 1 \qquad (1.2)$$

where σ_1 and σ_2 are principal stresses and σ_{ut} and σ_{ue} are ultimate tensile and compressive strength. The modified maximum strain energy theory

$$\left(\frac{\sigma_1}{\sigma_{ut}}\right)^2 - 2\nu\left(\frac{\sigma_1\ \sigma_2}{\sigma_{ut}\ \sigma_{ue}}\right) + \left(\frac{\sigma_2}{\sigma_{ue}}\right)^2 = 1 \qquad (1\text{-}3)$$

where ν is the poisson's ratio, appears to serve as an upper bound.

CHAPTER II

WEAKEST-LINK STATISTICS AND WEIBULL THEORY

In this introductory presentation, the concept of 'weakest-link' statistics for fracture [17] due to tensile stresses has been used to develop this theory of probability. Consider a volume V of the material which has the property that fracture of a sub-volume v will cause catastrophic failure of the whole. V is assumed to be much larger than v. For generality and simplicity elemental volumes v_i are assumed to be equal and cubic. Each of the elemental volumes will fracture at certain stress σ, characterstic of that element, and we assume a statistical distribution of these strengths.

The probability density function for the elemental volumes is designated $f(\sigma)$. It can be defined in the following way: from an extremely large number of elemental volumes, the fraction will fail between σ and $\sigma+d\sigma$ is $f(\sigma)d\sigma$ which is the same as the probability that failure will occur between σ and $\sigma+d\sigma$. (Figure 2.1).

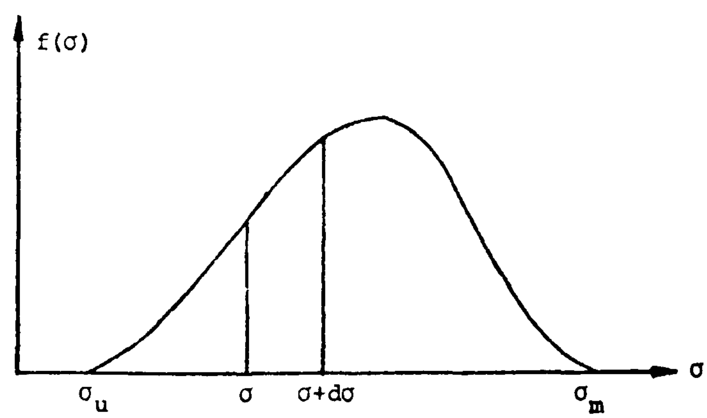

Figure 2.1. Probability Density Function, $f(\sigma)$

The probability that failure will occur before stress σ is reached is:

$$g(\sigma) = \int_{o}^{\sigma} f(\sigma)\,d\sigma \tag{2.1}$$

The probability that failure will occur before an infinite stress is reached is certain, that is, a probability of 1. This means that the function must be normalized such that:

$$\int_{o}^{\infty} f(\sigma) = g(\infty) - g(0) = 1 \tag{2.2}$$

thus the probability that the elemental volumes will survive a stress σ is:

$$1 - g(\sigma) \tag{2.3}$$

In the weakest link model, Figure 2.2 the volume V is imagined composed of a large number N of elemental volumes v, then the number of elements is $N = V/v$. It is now assumed that the failure of one element causes the failure of the whole. The probability of failure of the whole in the stress range σ to $\sigma + d\sigma$ due to failure of one element is the probability of failure of that element $f(\sigma)d\sigma$, multiplied by the probability that N-1 elements survive $\left\{1 - g(\sigma)\right\}^{N-1}$.

Thus, probability of this occurrence is the product of the probabilities:

$$f(\sigma)\,d\sigma \left\{1 - g(\sigma)\right\}^{N-1} \tag{2.4}$$

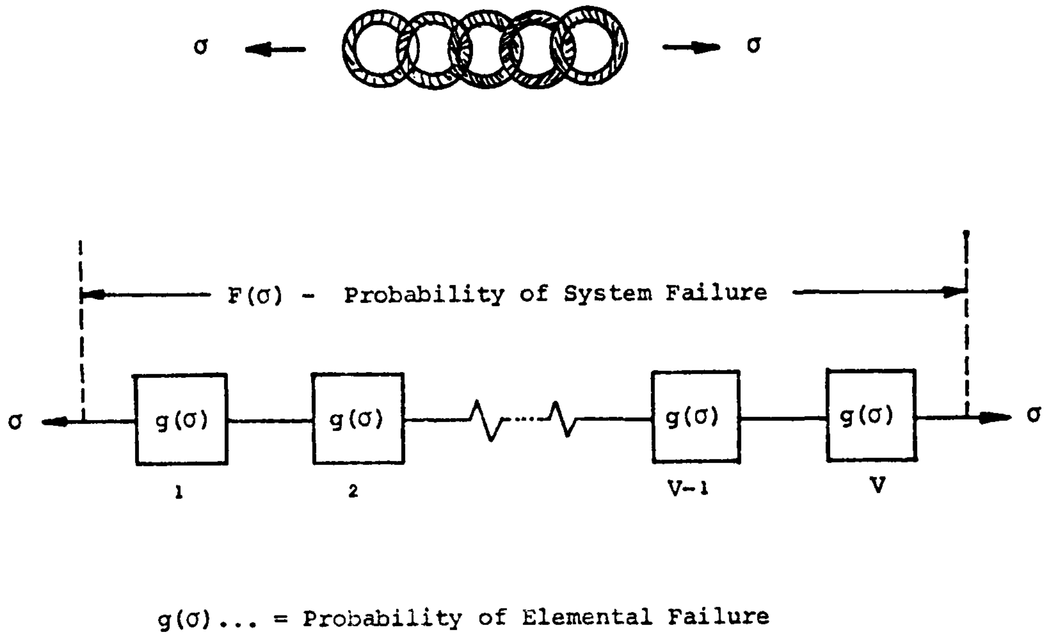

Figure 2.2. The Weakest-Link Model

On the other hand two breaks might occur simultaneously with the probability:

$$f(\sigma)^2 d\sigma^2 \left\{1 - g(\sigma)\right\}^{N-2} \tag{2.5}$$

but such simultaneous events are very rare and can be neglected. Thus the probability density function for the volume V consisting of N elements is proportional to:

$$P(\sigma) \propto f(\sigma) \left\{1 - g(\sigma)\right\}^{N-1} \tag{2.6}$$

The elements that fail could be any one of the N elements, thus:

$$P(\sigma) = Nf(\sigma) \left\{1 - g(\sigma)\right\}^{N-1} \qquad (2.7)$$

For large N and small g, the Poisson approximation is good. $(1 - g)^N \simeq e^{-Ng}$ which can be seen from the Taylor expansions of the left and right sides:

$$(1-g)^N = 1-Ng + \frac{N(N-1)g^2}{2} - \frac{N(N-1)(N-2)g^3}{3} + \ldots\ldots$$

$$e^{-Ng} = 1-Ng + \frac{N^2g^2}{2} - \frac{N^3g^3}{3} + \ldots\ldots \qquad (2.8)$$

also for large N, $(N-1) \simeq N$ to make:

$$P(\sigma) \simeq Nf(\sigma)(1-g)^{N-1} \simeq Nf(\sigma)\, e^{-Ng} \qquad (2.9)$$

Again normalization predicts certain failure for an infinite stress, giving:

$$\int_0^\infty P(\sigma)\,d\sigma = 1 \qquad (2.10)$$

Now the probability of failure function for the volume V comprised of N elements can be written from eq. 2.9. It has the general shape

$$F(\sigma) = \int_0^\sigma P(\sigma)\,d\sigma = N\int_0^\sigma e^{-Ng} f(\sigma)\,d\sigma \qquad (2.11)$$

given by that of Figure 2.3

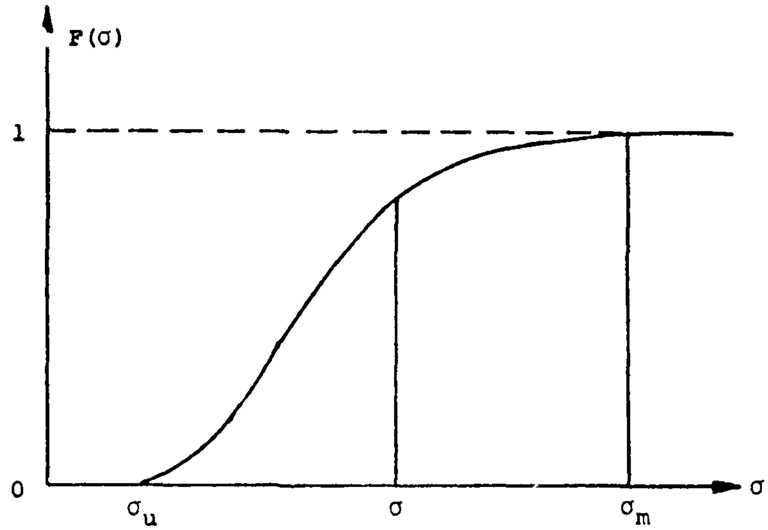

Figure 2.3. Cumulative Distribution Function, F(σ)

Equation 2.9 gives the normalized probability density function and equation 2.11 is the basic failure probability for weakest link statistics.

If we consider the experimental strengths obtained from a series of specimens, we will find that there is a definite relationship between the probability that a specimen will fracture and the stress to which it is subjected. This relationship is often called the distribution function of the strength. Every specimen has a unique distribution function. In other words, the distribution function is dependent upon the size and design of the specimen. Many different functions have been assumed for g, the failure probability for the elements. The one that is simple mathematically, agrees with a wide variety of experimental data, covering not only material strengths but many other statistical data [12] and which appears physically

reasonable when the use of it in the above statistics is examined, is the Weibull distribution.

$$\left.\begin{array}{ll} g(\sigma) = \left(\dfrac{\sigma - \sigma_u}{\sigma_o}\right)^m & \sigma_u + \sigma_o > \sigma \geq \sigma_u \\ g(\sigma) = 1 & \sigma \geq \sigma_u + \sigma_o \\ g(\sigma) = 0 & \sigma < \sigma_u \end{array}\right\} \qquad (2.12)$$

Notice that when $\sigma < \sigma_u$, there is no probability of failure. This is the 3-parameter distribution. Some researchers assume $\sigma_u = 0$ because this leads to helpful simplifications in the application of Weibull statistics to experiments [18]. A typical distribution curve of strength [19] for $\sigma_u = 0$ is shown in the Figure 2.4. This lower bound σ_u on the strength of the element is also the lower bound for the large volume. σ_u must be found for the particular material and for the failure mode being considered, by experiment. Because the greatest value a probability of failure function can have for the element is 1, $\left((\sigma - \sigma_u\right)/\sigma_o)^m$ can not represent this function beyond a certain value of σ. That value is found from the equation:

$$g(\sigma_{max}) = \left(\frac{\sigma - \sigma_u}{\sigma_o}\right)^m = 1 \qquad (2.13)$$

This will occur when $\sigma_{max} = \sigma_u + \sigma_o$, therefore we have put $g(\sigma) = 1$ for $\sigma \geq \sigma_u + \sigma_o$. Thus $\sigma = \sigma_u + \sigma_o$ is the greatest strength the elemental volumes could have if the Weibull statistics were valid over the range $\sigma_o \leq \sigma \leq \sigma_u + \sigma_o$. However it is only the lower tail of g that is effective in 'weakest-link' statistics, and it is

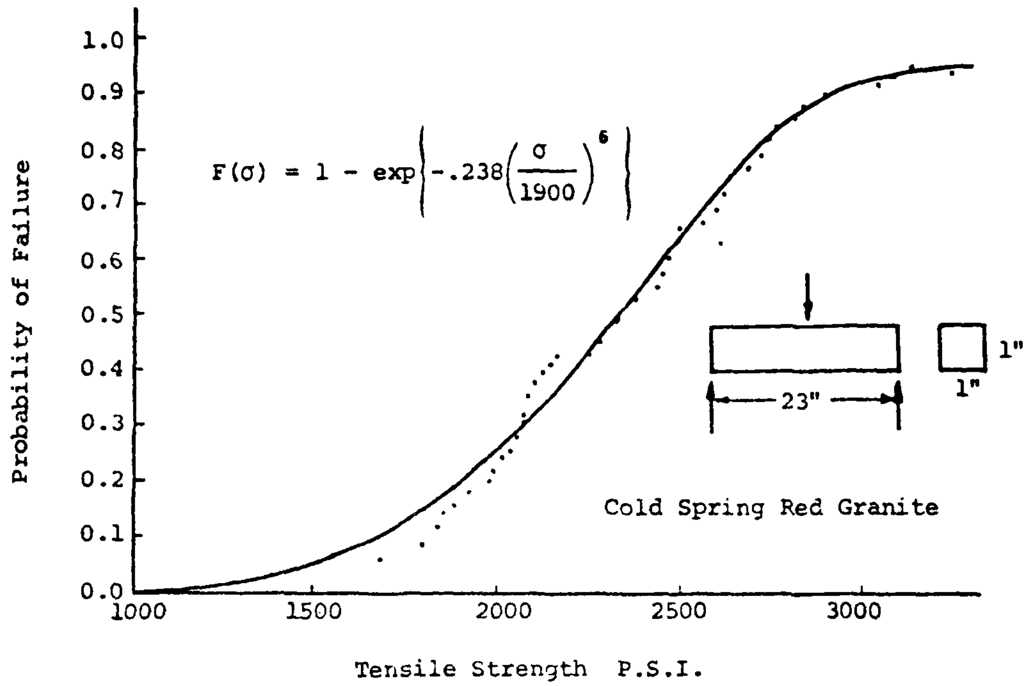

Figure 2.4. A Weibull Distribution of Tensile Strengths (Source: Hudson, J.A. and Fairhurst, Charles, "Tensile Strength, Weibull's Theory and A General Statistical Approach to Rock Failure.")

reasonable that another simple power function could be fitted to the data in this limited region. Using Eq. 2.11 and 2.12 now the probability of failure for the volume V comprised of N elements can be written as:

$$F(\sigma) = 1 - \exp\left|-N\left(\frac{\sigma - \sigma_u}{\sigma_o}\right)^m\right| \qquad (2.14)$$

Since volume V is proportional to number of elements, N, Eq.(17) can be written as:

$$F(\sigma) = 1 - \exp\left|\frac{-V}{V_{un}}\left(\frac{\sigma - \sigma_u}{\sigma_o}\right)^m\right| \qquad (2.15)$$

A simple example can show how only the lower tail of the distribution function, g, is important. Consider a sample of 100*100*100 elements. Thus $N = 10^6$. A typical value for the exponent m is 5. Let us calculate the probability that failure for a volume in the lower 1/10 of the strength range of each element, stressed uniaxially and uniformly. Inserting $\sigma = \sigma_u + 1/10(\sigma_o)$ into Eq. 2.14 the probability of failure function, using $V/v_{un}=10^6$ is:

$$F(\sigma) = 1 - \exp\left| - 10^6 \left(\frac{1}{10}\right)^5 \right| \tag{2.16}$$

$$= 0.999954$$

Thus the probability of failure is almost 1 even though the threshold stress was exceeded only by $\sigma_o/10$. Consequently the shape of $f(\sigma)$ and $g(\sigma)$ beyond $\sigma + \sigma_o/10$ is of little interest.

WEIBULL'S THEORY

Weibull's statistical theory is based on the 'weakest-link' concept. The fact the term 'weakest-link' is used because the same statistics apply to a chain whose strength is described as the strength of its weakest link. In other sense, if N seemingly identical specimens are broken in identically the same way, it is quite possible that no two would fracture at the same load. Instead, they can show a variability of 100% or more; however, the greater portion most probably would fracture within a narrow range of loads, which leads one to believe that the strength of a material might lend itself to statistical treatment. To relate the model of a chain to that of a tension specimen one must imagine a multitude of fibers, each acting like a chain, it can be shown that the probability that a model specimen of this type will fracture at a certain load is a function of its volume [20].

As has been pointed out above, a specimen may be considered to be made up of many fibers. Each of these fibers can be considered as having its own probability of withstanding a load, but the probability for the entire specimen will be the result of considering the individual probabilities of all the fibers. Giving an example of bending specimen, one-half of the fibers in the test volume will be in tension, and the remaining fibers will be in compression. Weibull's theory assumes that fibers in compression have a zero probability of failure. As a result, these compressed fibers do not contribute to the probability for the entire specimen. Therefore, an entire half of the specimen is neglected in Weibull's consideration of the probability

of a specimen's withstanding a bending load. But in considering the probability of a specimen's withstanding a load, every fiber must be considered.

Using this concept the Weibull distribution function for predicting the probability of failure is expressed as:

$$F(\sigma) = \begin{cases} 1 - \exp\int_V - \left(\frac{\sigma - \sigma_u}{\sigma_o}\right)^m \frac{dV}{V_{un}} & \sigma_u < \sigma \leq \sigma_u + \sigma_o \\ 0 & \sigma \leq \sigma_u \end{cases} \qquad (2.17)$$

V is the volume of the material under a uniaxial stress σ. Generally σ may be a function of the volume, in which case F will be a function of the external loading parameters.

The above Weibull distribution function describes the behavior of many simple and important load carrying elements. For a tension member under a constant stress state, the above distribution function can also be expressed as follows:

$$F(\sigma) = 1 - \exp\left\{-c(\sigma - \sigma_u)^m\right\} \qquad (2.18)$$

where $c = \dfrac{1}{V_{un}(\sigma_o)^m}$

and:

V_g = Gage volume of the material

V_{un} = Unit volume of material

σ = Applied uniform tensile stress

F = Probability of failure

σ_u = Threshold stress below which there is zero probability of fracture

m = Distribution constant or Weibull modulus

c = Constant

σ_o= A free parameter needed to fit the function to the data

σ_u, m, and σ_o (or c) are material constants.

Parameters σ_u, m, and σ_o are material constants in the true sense and will not change with volume provided the Weibull function is truly applicable to the material under consideration, and if the materials used for small test specimens and for the structural components are truly identical. However, σ_o or c is merely a normalizing factor and is not otherwise related to any physical property of the material. The value of m is a measure of the strength variability or scatter and it helps in determining whether the material contains flaws of highly variable severity or similar geometry [21].

Estimation of Weibull parameters from experimental data is a very important step in the determination of material characteristics. A large number of methods are in use to obtain Weibull parameters. Heavens and Murgatroyd [22] in their work used the methods of linearization, direct curve fitting, and maximum likehood. The problem is complicated by the fact that no method can be proved to be best under all circumstances. One can, for example, estimate the mean of a normal distribution by taking the arithmatic average or by finding the most frequently occuring value of the data. Davies [23] has suggested another method for the estimation of Weibull parameters. This method equates the mean variance and higher moments of the distribution of those of observed data. Another technique for finding these parameters is based on the moment generating method and on rank-order theory [24,25].

These results differ from those obtained by iteration methods whereby the sums of squares of deviations are minimized as is the case of standard least-square techniques. A detailed explanation of such methods have been given in Appendices A and B. These methods can involve large truncation errors and can be significantly less precise than comparison with cumulative totals (Histogram Method for the Solution of Weibull Parameters) of experimental data (Appendix C). Further, although the least-square analysis method tends to emphasize deviation in the experimental curve ordinates, incorporation of appropriate weights can counter this effect while preserving the method's basic simplicity.

Another problem with these techniques is that an assumption is generally required for multiaxial stress states necessitated by the uniaxial stress state under which data is taken. Many persons assume statistical independence in the actions of principal direction stresses, i.e., the probability of failure of an element is equal to the product of probabilities of failure due to each principal stress [26, 27]. Under three principal direction stresses the probability of failure is given by:

$$F(\sigma) = [F(\sigma_1)]\,[F(\sigma_2)]\,[F(\sigma_3)] \tag{2.19}$$

In another theory, Batdorf and Cross [28] and Batdorf [29, 30] assumed flaws to be penny-shaped and neglected the shear on the crack plane. Fracture of a crack was assumed to depend only on the components of stress state normal to the crack plane. Freudenthal [21] and Margetson [14] extended Weibull's uniaxial theory for stress assuming

that cracks obey the assumptions of independence and shear insensitivity. Evans [31] developed a theory for statistical analysis of fracture under multiaxial states of stresses based on a critical coplaner strain-energy release-rate fracture criterion.

Because a satisfactory and general treatment is not available in the literature particularly for the three-parameter family, an analytical method based on the same least-square method using an iterative programming scheme is developed. The objective is to find those values of Weibull parameters which make the theoretical curve fit the experimental data best for the Weibull's materials subjected to various states of stress. The methodology thus developed is illustrated by applying it to two sets of man-made data (Chapters III and IV). Additional properties of Weibull statistical distribution are given in Appendix D, including a Goodness-of-Fit analysis test that supplements topical material of this Chapter.

CHAPTER III

DEVELOPMENT OF SIMPLE TEST ANALYSIS CASES

Weibull's classical statistical theory includes two basic criteria of failure; size and normal tensile stress. Within the validity of these postulates it is capable of describing failure for any type of stress distribution, uniform or non-uniform, uniaxial or polyaxial. Failure in an isotropic and homogenous material is more fully described by the three-parameter family than by the two-parameter family. No special allowance is made for nonuniformity of stress distribution other than that implied in the integration procedure, Eq. 3.1 . Daniel and Weil [32, 33] used standard specimen shapes to generate Weibull statistics for some typical cases of bending loading conditions. The three-parameter family is developed here - first for uniaxial case.

Uniaxial Constant Stress Fields and the Determination of Weibull Parameters

The Weibull distribution for a uniaxial stress field in a homogenous isotropic material at a given uniform stress, σ is given by:

$$F(\sigma) = \begin{cases} 1 - \exp - \int_V \left(\frac{\sigma - \sigma_u}{\sigma_o} \right)^m \frac{dV}{V_{un}} & \sigma_u < \sigma \leq \sigma_u + \sigma_o \\ 0 & \sigma < \sigma_u \end{cases} \quad (3.1)$$

where: V_{un} = Unit Volume

σ_u, σ_o, m = Weibull paramters which are associated with the material and are independent of size.

For uniaxial constant stress, σ is a principal stress, independent of the volume so that :

$$F(\sigma) = 1 - \exp\left\{ - \frac{V_g}{V_{un}} \left(\frac{\sigma - \sigma_u}{\sigma_o} \right)^m \right\} \tag{3.2}$$

substituting $$c = \frac{1}{V_{un} (\sigma_o)^m}$$

$$F(\sigma) = 1 - \exp\{- c(\sigma - \sigma_u)\}V_g \tag{3.3}$$

The first solution procedure (the Log-Log method) is based on linear regression method which converts the exponential type Weibull distribution function into a straight line relationship by taking the log of the distribution function twice, thus:

$$\ell n \ell n \left(\frac{1}{1 - F(\sigma)} \right) = \ell n(c) + m \, \ell n(\sigma - \sigma_u) \tag{3.4}$$

This is now a linear relationship allowing a linear least-square analysis to be invoked for :

$$Y = A + Bx$$

$$\text{where } A = \ell n(c)$$

$$\text{and } B = m \tag{3.5}$$

$$\text{If } X_i = X(\sigma_i) = \ell n(\sigma_i - \sigma_u)$$

$$\text{and } Y_i = Y(\sigma_i) = \ell n \ell n \left(\frac{1}{1 - F(\sigma_i)} \right) \tag{3.6}$$

i = 1, 2, 3 ..., n, where n is the number of data points. Then A, B are constants, which must be determined, using the least-square criterion. The well known solution that minimizes the residual is:

$$A = \frac{(w_i\ X_i^2)\ (\Sigma w_i\ Y_i) - (\Sigma w_i\ X_i)\ (\Sigma w_i\ X_i Y_i)}{D}$$

$$B = \frac{(\Sigma w_i\ Y_i\ X_i)\ (\Sigma w_i) - (\Sigma w_i\ X_i)\ (\Sigma w_i\ Y_i)}{D} \tag{3.7}$$

where:

$$D = (\Sigma w_i)\ (\Sigma w_i\ X_i^2) - (\Sigma w_i\ X_i)^2$$

w_i = Arbitrary weights assigned to data points

All summations are i = 1, 2, ..., n.

In case equal weights are desired, the quantity Σw_i is replaced by n. The obvious difficulty with this analysis is that A and B are dependent on σ_u. To determine the best σ_u value, an iterative programming scheme, computer program, UNIAX.FOR, was developed which recomputes the residual sum of squares and chooses σ_u minimizing this function. Once σ_u is known, m is determined as the slope of the straight line expression and c is found as exp(A) in Eq. 3.5. A slight modification this scheme can be used to redefine the weights iteratively to emulate any curve-fitting power law. This would allow the simplicity of the least-square solution to be invoked while the weights are dynamically altered to (1) emphasize the leading distribution data or (2) de-emphasize errant points. Standard least-square techniques have the disadvantage of emphasizing any point away from the curve by squaring that deviation.

Comparison Methods

As discussed earlier, other techniques exist to determine the Weibull parameters from the series of data obtained from the experimental tests. As an example, the results from the Moment Generating Method (Appendix A) and the Newton-Raphson iteration (Least-square) method are compared with those obtained from the Log-Log Method.

Table 3.1 demonstrates that while a surprising discrepancy can exist in the values of the Weibull parameters (c, m, σ_u), the overall probabilities can appear very close -- at least in the mid-range. In the lower range, however, the probabilities can differ greatly. Unfortunately, this range is of major interest in dealing with materials where the test elemental volume is small in comparison to the volume of the structure being modeled. (All weights were assumed unity for this example.)

Pure Bending Field in a Rectangular Section Bar

In the application of brittle non-metallic materials, tests utilizing bending stress distributions to failure on small, rectangular cross-section bars are common and generally less expensive than uniaxial tension tests -- particularly, in the case of three and four point loading systems. In the latter case, the central portion of the bar is subjected to a constant bending moment. Applying the Weibull expression [32, 18, 34], where the stress distribution is variable and must be integrated over the volume in bending, the probability of failure in the pure bending section of a uniform prismatic beam, simply-supported and loaded as in Figure 3.1 is:

$$F(\sigma) = 1 - \exp\left\{ - \frac{V_g}{V_{un}} \left(\frac{\sigma - \sigma_u}{\sigma_o} \right)^m \right\}$$

$$V_g = .125 \text{ in.}^3$$

σ k.s.i.	RANK i	$F(\sigma) = \frac{i}{n+1}$	$F(\sigma)$ M.G.Method	$F(\sigma)$ N-R Method	$F(\sigma)$ L.L.Method
7.55	1	0.0625	0.0279	0.0362	0.0618
8.55	2	0.1250	0.0592	0.0653	0.0970
10.91	3	0.1875	0.1979	0.1913	0.2258
11.60	4	0.2500	0.2555	0.2453	0.2757
12.44	5	0.3125	0.3338	0.3208	0.3429
13.50	6	0.3750	0.4414	0.4284	0.4353
13.65	7	0.4375	0.4570	0.4444	0.4489
14.00	8	0.5000	0.4937	0.4823	0.4808
14.75	9	0.5625	0.5716	0.5643	0.5497
14.83	10	0.6250	0.5798	0.5730	0.5571
15.96	11	0.6875	0.6902	0.6921	0.6583
16.41	12	0.7500	0.7304	0.7359	0.6966
16.60	13	0.8125	0.7465	0.7535	0.7122
20.00	14	0.8750	0.9409	0.9575	0.9190
21.50	15	0.9325	0.9755	0.9866	0.9631

WEIBULL PARAMETERS	M.G. Method	N-R Method	L.L. Method
c (in.$^{2m-3}$ k.s.i.$^{-m}$)	0.0007079	0.00002329	0.00003219
m (dimensionless)	3.0	4.03	3.76
σ_u (k.s.i.)	4.13	1.35	0.026
σ_o (k.s.i.)	5.61	14.11	15.67
RESIDUES (dimensionless)	0.028309	0.026618	0.038729

Table 3.1. A Comparison of Methods of Determining Weibull Parameters

$$F(\sigma_b) = 1 - \exp\left[- \left\{ \frac{V}{2(m+1)} \left(1 - \frac{\sigma_u}{\sigma_b}\right) \left(\frac{\sigma_b - \sigma_u}{\sigma_o}\right) \right\}^m \right] \qquad (3.8)$$

where V = bLh

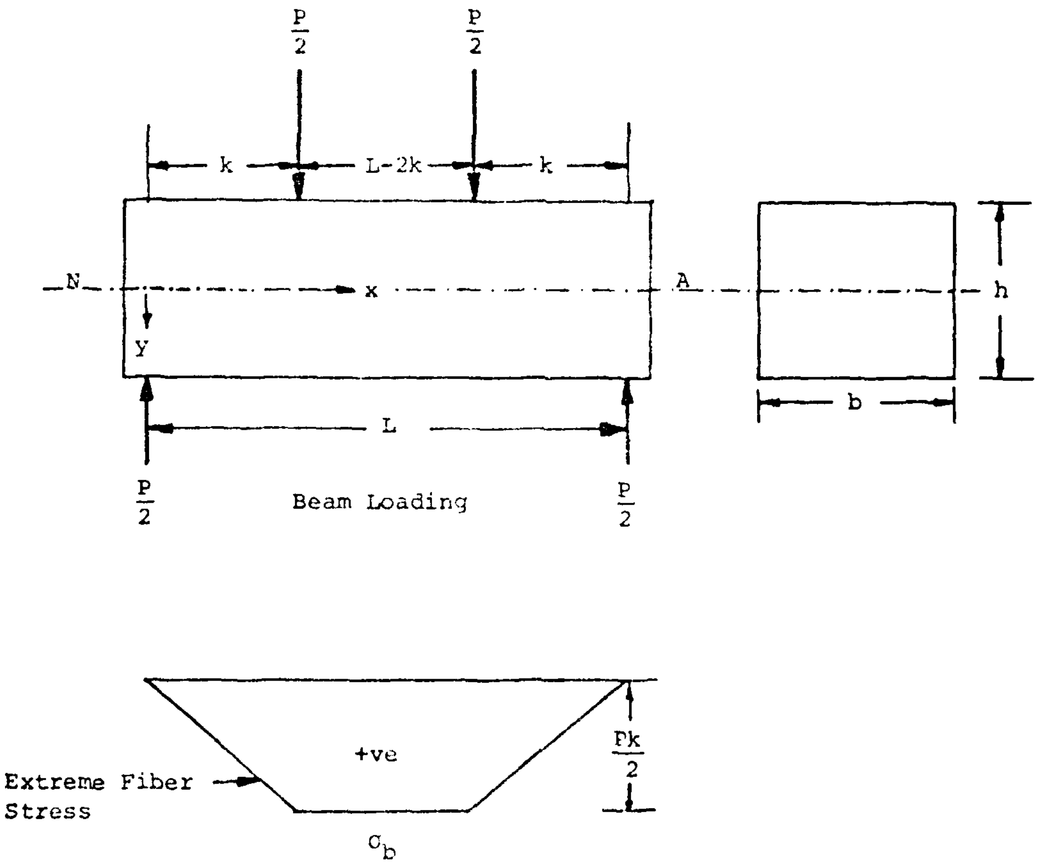

Beam Loading

Bending Moment Diagram

Figure 3.1. Prismatic Beam under 4-Point Loading and Distribution of Extreme Fiber Stress

Both support and loading points are symmetrically positioned about the beam center. The risk of rupture in the outer portion of the specimen has been neglected in Eq.(3.8) but it is easily included. Fig. 3.1 depicts this case with its gage volume equal to the pure bending segment. The distribution of tensile stresses in central portion of the test volume subjected to uniform bending is:

$$\frac{\sigma}{\sigma_b} = \frac{2y}{h} \quad ; \quad \sigma = \frac{2\sigma_b y}{h} \tag{3.9}$$

$$\text{for } k \leq x \leq (L-k)$$

where σ_b, the extreme fiber stress at bottom, for a 4-point loading is given as:

$$\sigma_b = \frac{3Pk}{bh^2} \quad ; \; P = \text{Fracture load} \tag{3.10}$$

This distribution follows the same form of the case of a constant uniaxial stress field and is solved by the same technique as with the uniaxial constant stress field except that different constsnts result when the log-log is taken in Eq. 3.8 instead of Eq. 312. The programming scheme is given in BENDIN.FOR, Appendix D, thus:

$$\ell n \ell n \left(\frac{1}{1 - F(\sigma_i)} \right) = \ell n(V/2) - \ell n(m+1) + (m+1)\, \ell n(\sigma_i - \sigma_u)$$
$$- \ell n(\sigma_i) - m\, \ell n(\sigma_o) \tag{3.11}$$

In this case;

$$A = \ell n(V/2) - \ell n(m+1) - m\, \ell n(\sigma_o)$$
$$B = (m+1) \tag{3.12}$$

with σ_u and m estimated, σ_o is calculated from the Eq. (3.12).

Pure Bending for a Circular Cross-Section Rod or Tube

This case is similar to the one discussed earlier, except that the shape of the cross-section is circular. Davies [35] in his work observed that any minor defects incurred during manufacture along the sharp edges of beam specimens of rectangular cross-section that could influence significantly the probability of failure. Beam specimens of circular cross-section have no sharp edges and are therefore an attractive alternative geometry.

Unfortunately the use of a simpler geometry specimen leads to the complication that no closed-form solution exists for the probability formulation in bending.

The stress distribution for the case of 4-point loading of a rod is:

$$\sigma = \frac{M\,y}{I} = \frac{2Pky}{\pi\,Ro^4} \quad ; \quad k \leq x \leq (L-k)$$

or for a tube:

$$\sigma = \frac{M\,y}{I} = \frac{2Pky}{\pi(Ro^4 - Ri^4)} \quad ; \quad k \leq x \leq (L-k) \qquad (3.13)$$

where P is the fracture load.

For the failure probability expression the integration is conducted over the gage volume, v_g, which is in pure bending. Starting from the integral form for the risk of rupture, Bn, Figure 3.2

$$Bn = \iiint \left(\frac{\frac{M\,y}{I} - \sigma_u}{\sigma_o} \right)^m \frac{dx\ dy\ dz}{V_{un}} \ . \qquad (3.14)$$

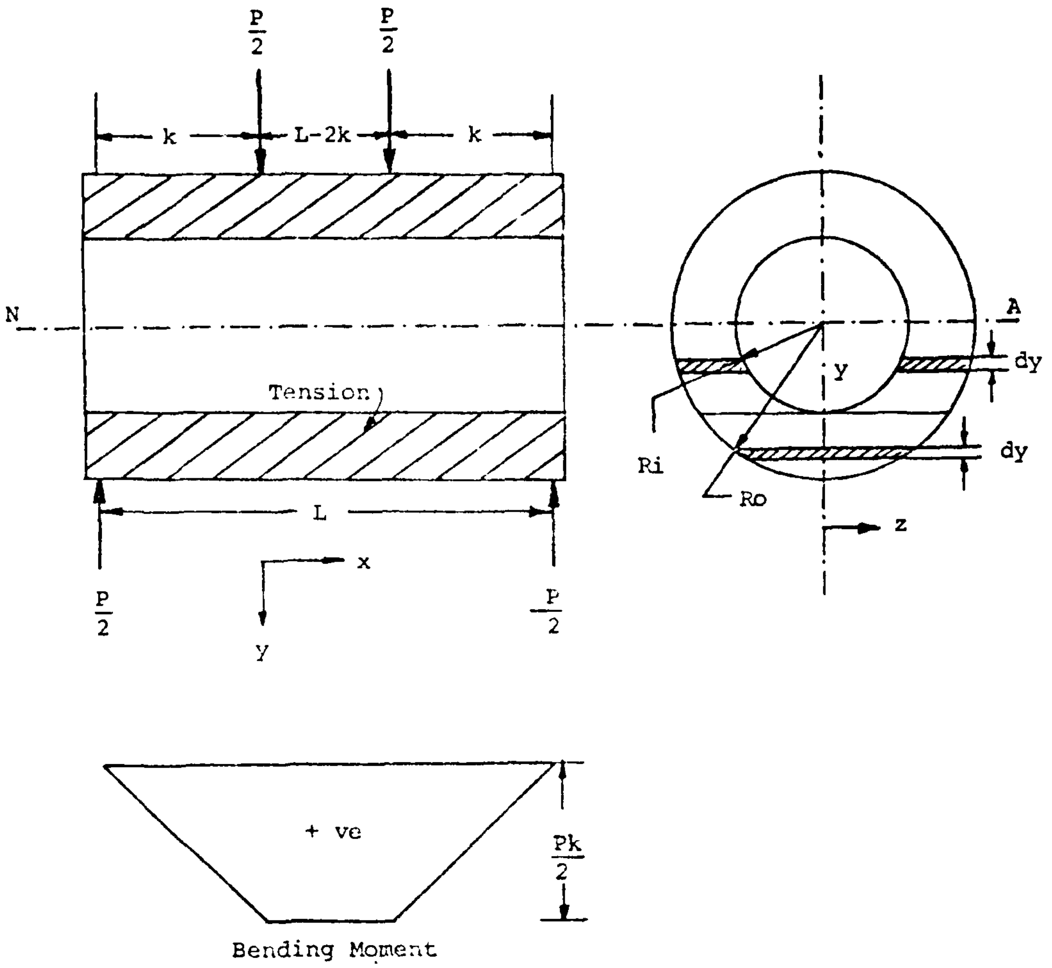

Figure 3.2. 4-Point Loading for a Circular Cross-Section Tube in Pure Bending

The limits of integration for x in Eq. 3.14 are 0 and (L-2k); thus:

$$Bn = (L-2k)c \iint_A \left(\frac{M\,y}{I} - \sigma_u \right)^m dz\,dy \qquad (3.15)$$

where $c = \dfrac{1}{V_{un}(\sigma_o)^m}$

The probability of failure is:

$$F(M) = 1 - \exp(-Bn)$$

The limits of integration for z and y in Eq. (3.15) **will be different in** different cases. These cases are considered as below.

(1) Rod (Ri=0)

(a) $0 \leq y_{th} < Ro$

Y_{th} is the positive value of y for which $\sigma = \sigma_u$, thus:

$$y_{th} = \frac{\sigma_u I}{M}$$

Parts of the cross-section for which $y < y_{th}$ make no contribution to Bn. For a fixed y such that $y \geq y_{th}$, the limits of integration for z are obviously;

$$-\sqrt{(Ro^2 - y^2)} \quad \text{and} \quad +\sqrt{(Ro^2 - y^2)}$$

Therefore,

$$Bn = (L-2k)c \int_{y_{th}}^{Ro} \int_{-\sqrt{(Ro^2 - y^2)}}^{+\sqrt{(Ro^2 - y^2)}} \left(\frac{M\,y}{I} - \sigma_u\right)^m dz\,dy \qquad (3.16)$$

integration of Eq. (3.16) with respect to z gives:

$$Bn = 2(L-2k)c \int_{y_{th}}^{Ro} \left(\frac{M\ y}{I} - \sigma_u\right)^m \sqrt{Ro^2 - y^2}\ dy \tag{3.17}$$

(b) $Ro \leq y_{th}$; In this case, obviously

$Bn = 0$

(2) Tube ($Ri \neq 0$): Three cases occur;

(a) $Ri > y_{th} \geq 0$; The expression for Bn becomes:

$$Bn = (L-2k)c \left[\int_{y_{th}}^{Ri}\int \left(\frac{M\ y}{I} - \sigma_u\right)^m dz\ dy + \int_{Ri}^{Ro}\int \left(\frac{M\ y}{I} - \sigma_u\right)^m dz\ dy \right] \tag{3.18}$$

For the first integral, the limits of integration for z, for fixed y, will be from

$$-\sqrt{(Ro^2 - y^2)} \quad \text{to} \quad -\sqrt{(Ri^2 - y^2)}$$

and then from

$$+\sqrt{(Ri^2 - y^2)} \quad \text{to} \quad +\sqrt{(Ro^2 - y^2)}$$

For the second integral, the limits of integration for z, for fixed y, will be from

$$-\sqrt{(Ro^2 - y^2)} \quad \text{to} \quad +\sqrt{(Ro^2 - y^2)}$$

Performing the integration gives:

$$Bn = 2(L-2k)c\left[\int_{y_{th}}^{Ri}\left(\frac{M\,y}{I} - \sigma_u\right)^m\left(\sqrt{Ro^2 - y^2} - \sqrt{Ri^2 - y^2}\right)dy\right.$$

$$\left. + \int_{Ri}^{Ro}\left(\frac{M\,y}{I} - \sigma_u\right)^m\sqrt{Ro^2 - y^2}\;dy\right] \qquad (3.19)$$

(b) $Ri \leq y_{th} < Ro$

Following the procedure used above gives:

$$Bn = 2(L-2k)c\int_{y_{th}}^{Ro}\left(\frac{M\,y}{I} - \sigma_u\right)^m\sqrt{Ro^2 - y^2}\;dy \qquad (3.20)$$

This expression is identical to that in the case of a rod, Eq.(3.17). In fact the case of a rod is obtained from this one by setting Ri = 0.

(c) $Ro \leq y_{th}$; Here obviously

$$Bn = 0 \qquad (3.21)$$

CHAPTER IV

DESIGN OF THE BENDING EXPERIMENT

A major objective of this contract was to design tests and test specimens that provided a large amount of information on fractive strength of brittle materials at low cost. As such, tests such as the uniaxial tension test were abandoned due to the need of specially fabricated specimens and equipment where small strain to failure ratios in ceramics are an important design consideration [36].

A four-point test fixture and tube specimen geometry were selected because:

1) A simple circular specimen geometry (solid or tubular) could be used without excess concern of stress concentrations of polygonal section specimens.

2) The geometry was an inexpensive one to emulate with virtually all potential specimen materials. In many cases, tubes are 'off-the-shelf' items.

3) Either smooth or rough surfaces could be tested.

4) Without great difficulty, necked down specimens if needed could be designed to fit the same test equipment. The need for such designs would be apparent if the frequency of failures at the load points is high.

5) Four-point loading was selected over three-point loading because it provided a large volume in the test region subjected to a known stress field.

Figure 4.1 demonstrates the geometry used for the four-point load test. The fixture components are:

A. Base

B. Specimen resting on ground rollers

C. Copper pads to reduce stress concentrations at bearing points

D. 1.25" - diameter alignment rods for stablizing upper load frame

E. Upper pivot arm with load roller and specimen grooved rollers

F. Top guide block above which load is applied

Figure 4.2 is an assembled view with specimen in place. Figures 4.3 and 4.4 depict the dimensions and material details of the loading frame system as finally employed. A load is applied at the top center of the top guide block through a Tinius Olsen universal testing machine. This machine is accurately calibrated for load although the rate of load can only be approximated. Within the machine, the fixture of Figure 4.2 is placed; loading rates were approximately 40 pounds per second.

During the design and building of the testing apparatus, there was a question as to what type of alignment mechanism should be used to locate the outer (lower) and the inner (upper) specimen support points so that no sliding frictional constraint would be imposed during deflection. Stanley [18] did account for such an effect as it applied to a two-parameter Weibull test when the coefficient of static friction between the specimen material and fixture were known. In this apparatus, the use of rollers, made friction of minimal concern. Ideally, the use of two 'formed' pads on rollers (one on the top and one on the bottom) would eliminate all non-self equilibrating frictional forces -- Figure 4.5.

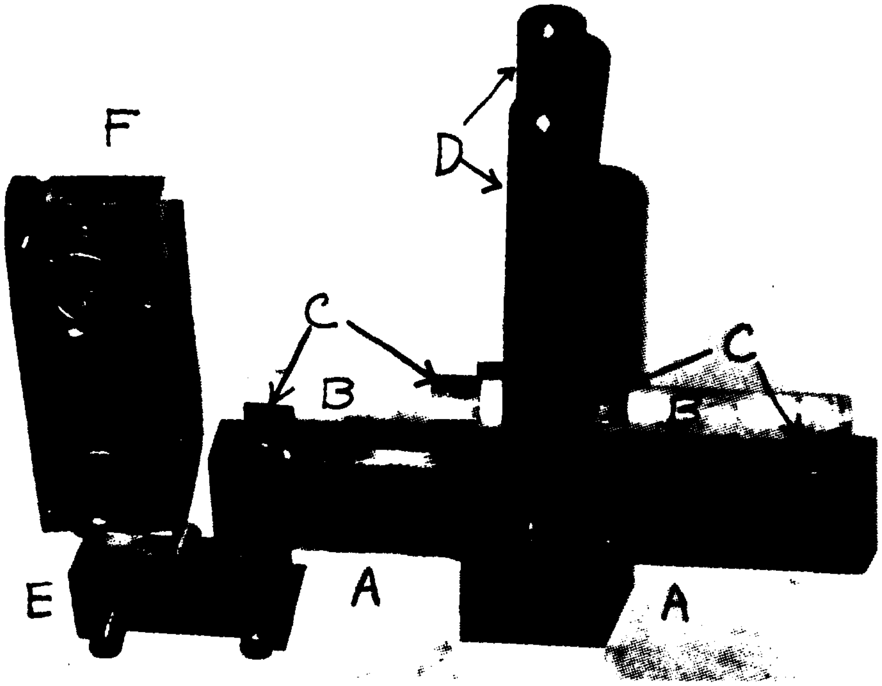

Figure 4.1. Components of Bending Test

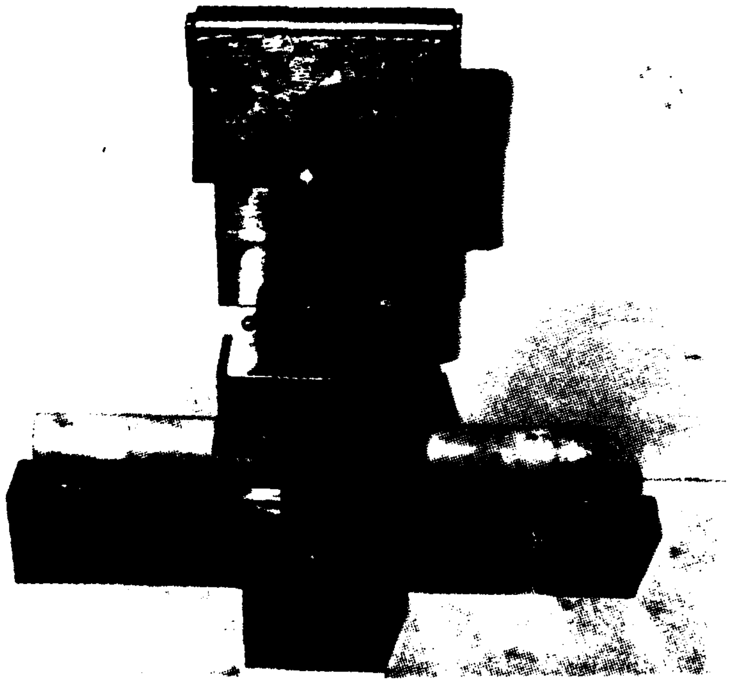

Figure 4.2. Assembled View of 4-Point Bend Test

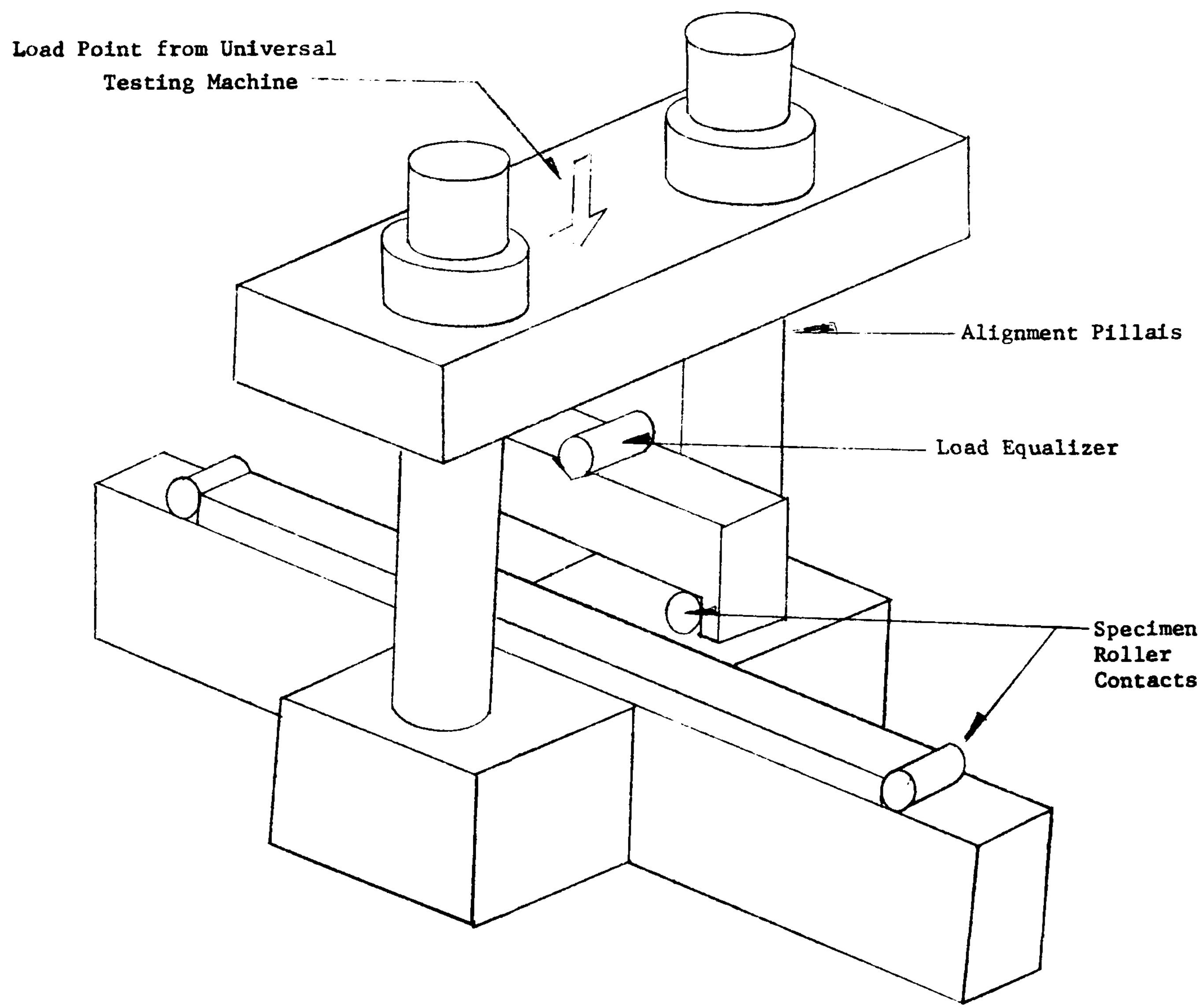

Figure 4.3. **Self Aligning 4-Point Bend Fixture - Assembled View Without Specimen**

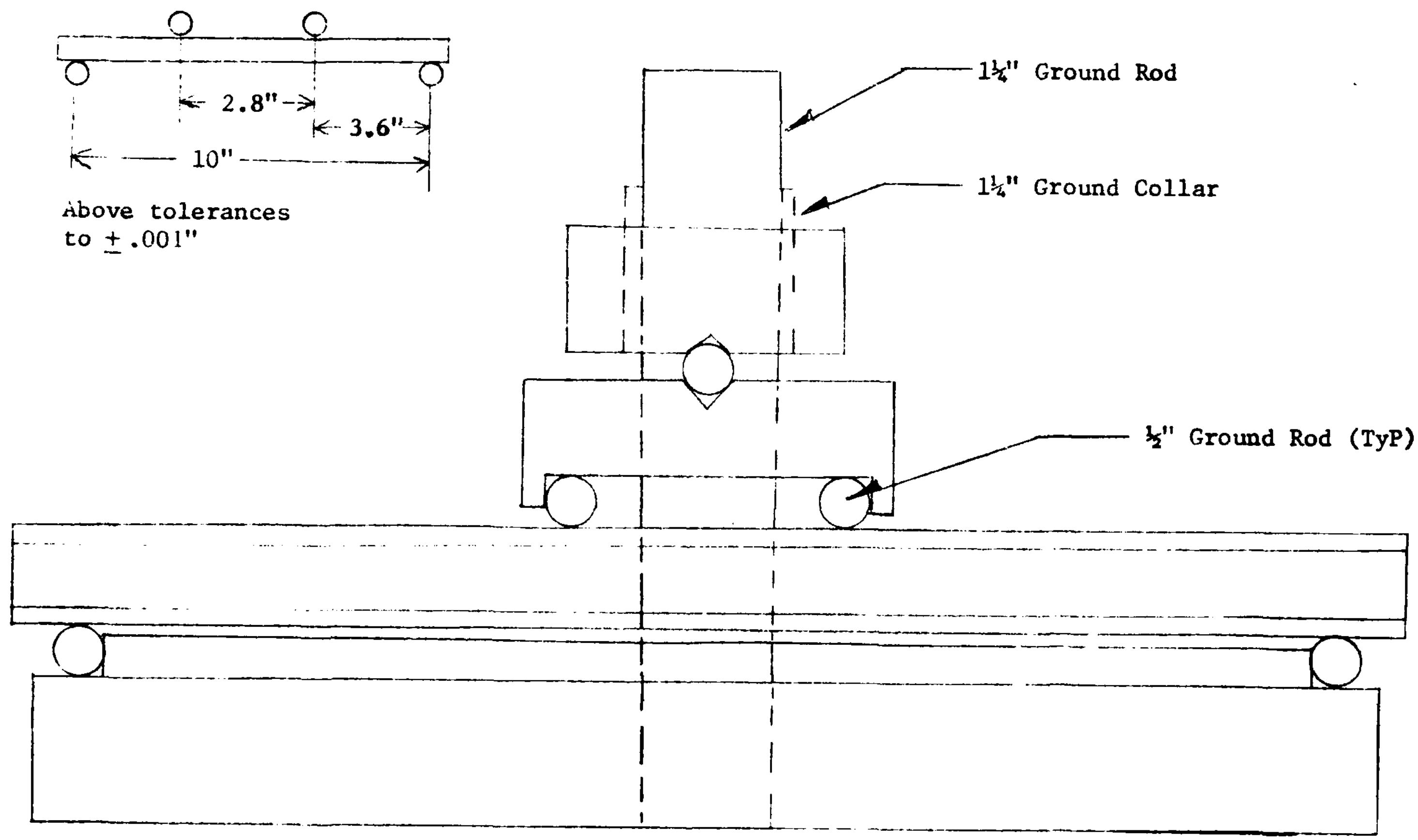

Figure 4.4. Dimensional Drawing of Bend Fixture

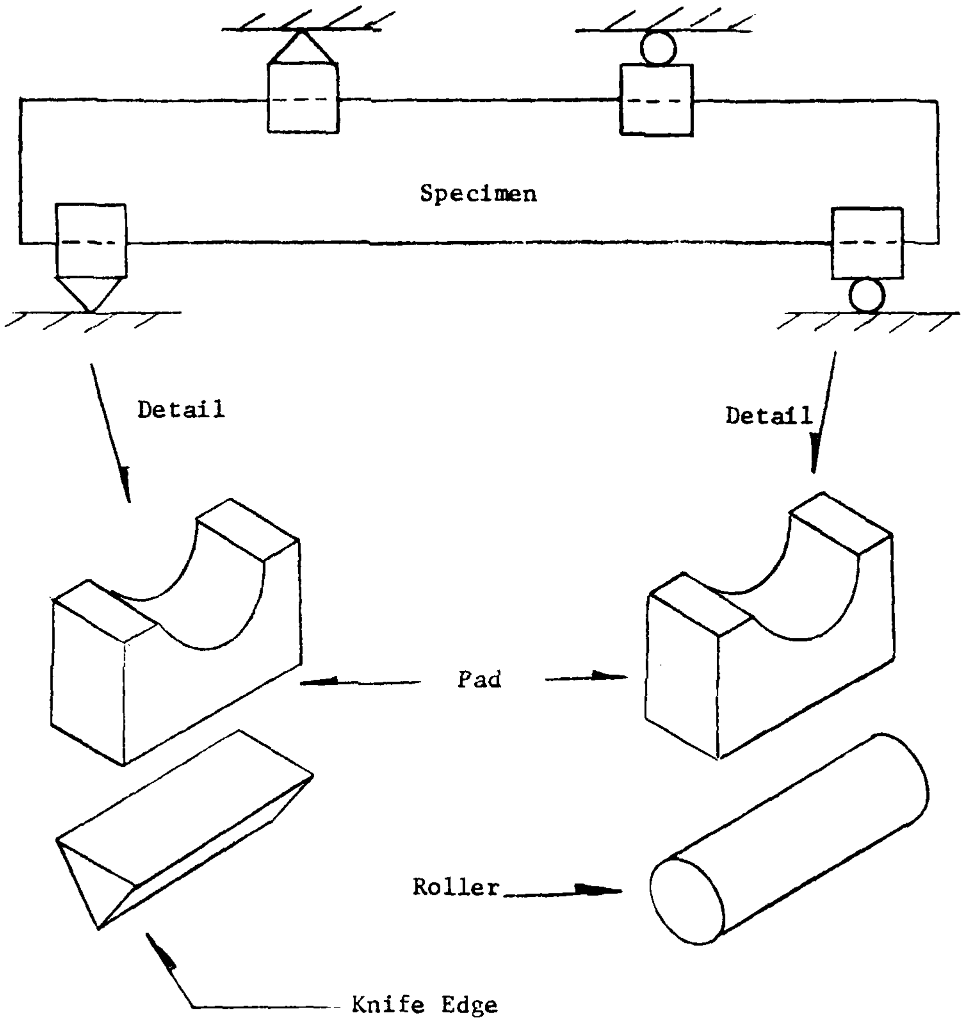

Figure 4.5. Pads and Roller Constraints

Of further concern was to determine a specimen contact design geometry so that no binding or specimen preload would be inadvertently imposed. The problem was to determine whether the apparent contraction due to bending at the lower points of support would offset the apparent elongation due to changes in slope at those same points. An approximation to this problem would be to determine whether A moves closer to or away from B. This would determine whether the geometry of Figure 4.6a or 4.6b would be appropriate for the base of a testing fixture for the specimen of Figure 4.3.

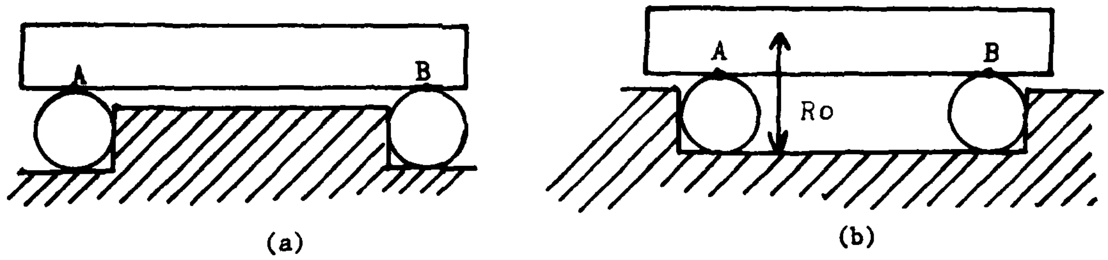

Figure 4.6. Possible Test Support Geometrics

To determine whether distance $\vec{AB}$ lengthens or shortens, first the contraction of the neutral axis must be found; it is given by:

$$\Delta L = \int_0^L (ds - dx) = \int_0^L \left(\sqrt{1+(y')^2} - 1\right) dx. \qquad (4.1)$$

for small slopes $|y'| << 1$, and $\sqrt{1+(y')^2} \simeq 1 + \frac{1}{2}(y')^2$ (4.2)

$$\Delta L \simeq \frac{1}{2}\int_0^L (y')^2 dx \qquad (4.3)$$

Thus, for a slender beam a contraction of any given span due to bending would always occur. However, the change in slope of a beam under load

tends to place the lower points of the beam in like curvature as indicated below in Figure 4.7.

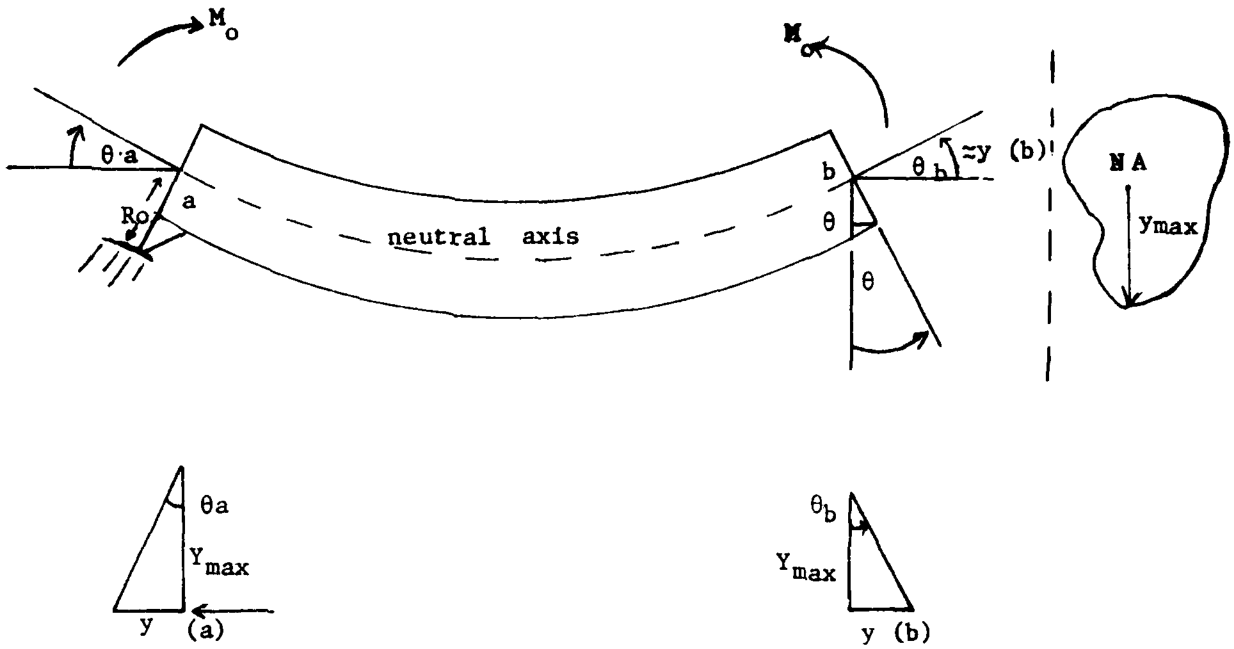

Figure 4.7. Bending Causing Outward Movement of Beam Lower Surface

Thus, the expansion or elongation between a and b is:

$$y_{max}\ [y^1(b) - y^1(a)] \sim \tfrac{1}{2}\int_0^L (y')^2 dx \qquad (4.4)$$

at the bottom of the beam [y_{max}] or at the total offset, Ro, wherever contact occurs.

In the case of a hollow rod in pure bending for its mid-length L, we have:

$$\tfrac{1}{2}\int_0^L (y')^2\, dx = \frac{M_o{}^2 L^3}{24E^2 I^2} \qquad (4.5a)$$

and

$$y_{max}[y^1(a) + y^1(b)] = \frac{R_o M_o L}{EI} \qquad (4.5b)$$

and one must check for $\dfrac{R_o M_o L}{EI} - \dfrac{M_o{}^2 L^3}{24E^2 I^2} \gtrless 0 \qquad (4.6)$

For the center span of a bar specimen in four-point loading, there is no need to perform a calculation to determine the geometry of the loading support as both the effect of slope and shortening of the neutral axis dictate that the Figure 4.6a is appropriate for the overall shortening.

Four-point loading, the above equation is an approximation to the change in distance between C and D of Figure 4.8 below provided $\ell \to \ell$ in length.

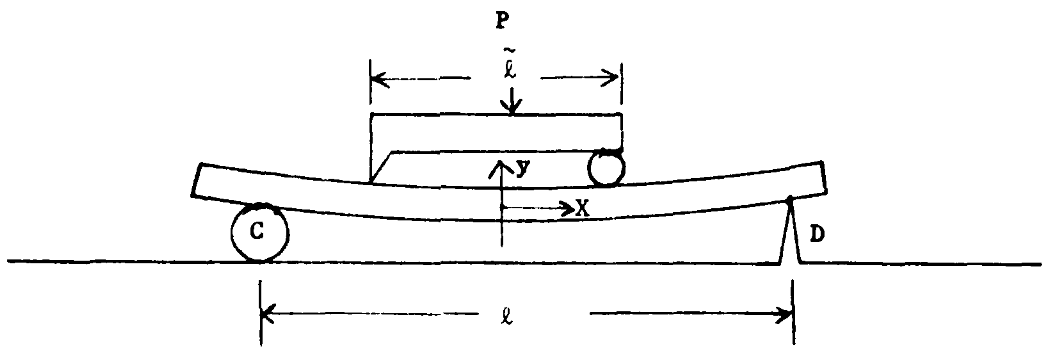

Figure 4.8. Bending Geometry and Notation

Thus, if $\tilde{\ell} \to \ell$ then from 4.5 and 4.6:

$$\frac{\tilde{L} M_O}{EI} \tilde{y} - \frac{1}{24} \frac{M_O^{2} \tilde{L}^{3}}{E^2 I^2} = d \tag{4.7}$$

Here y is the distance from neutral axis to point of support and

$$M_O = \text{Constant} = \frac{P(\ell - \tilde{\ell})}{4} \tag{4.8}$$

The exact solution is obtained by substitution of the moment distribution along the entire beam into (4.4) and integrating. In this case:

$$EI\ y^{1}(x) = \frac{P}{4}\ [<x+m>^{2} - <x+\tilde{m}>^{2} - <x-\tilde{m}> - (m-\tilde{m})(m+\tilde{m})]$$

$$\text{where}\quad m = \ell/2,\ \tilde{m} = \tilde{\ell}/2 \text{ and } <x - x_o>^{2} = \begin{cases} (x - x_o)^{2} & \text{if } x \geq x_o \\ 0 & \text{if } x < x_o \end{cases} \qquad (4.9)$$

Substitution of EIy"(x) derived from (4.9) and integration of each of the resulting expressions leads to:

$$\Delta L = \frac{1}{60}\left(\frac{P}{4EI}\right)^{2} [32m^{5} - 80m^{3}\tilde{m}^{2} + 80m\tilde{m}^{4} - 32\tilde{m}^{5}] \qquad (4.10)$$

for the beam in 4-point loading.

The slopes at the outer supports are given by:

$$y'(-m) = -\frac{P}{4EI}\ (m^{2} - \tilde{m}^{2})$$

and (4.11)

$$y'(m) = \frac{P}{4EI}\ (m^{2} - \tilde{m}^{2})$$

Thus, if the specimen is supported at an offset of R from the neutral axis, Figure 4.4a and b , then the restraining geometry Figure 4a should be used if $X > o$, otherwise 4b should be used where:

$$X = \frac{2P}{4EI}\ (m^{2} - \tilde{m}^{2})R_{o} - \frac{1}{60}\ \frac{P}{4EI}^{2} (32m^{5} - 80\ m^{3}\tilde{m}^{2} + 80m\tilde{m}^{4} - 32\tilde{m}^{5}) \qquad (4.12)$$

Thus, the specimen loading design is chosen with attention to several important details. By the use of bearings at the load points, the effect of friction is minimized and proper definition of the loading frame geometry (Figure 4.4a and b) eliminates a chance of superposition of compression in the test. Finally, there is a complicated stress field in

vicinity of the four loading areas. Machined surfaces on the test fixture at such points and soft copper pads reduced this problem, particularly, near the two inner contact points adjoining the gage length.

EXPERIMENTAL DETAILS

Specimens and Material

All specimens used in the experimental work were tubes of circular cross-section made of 99.8% Aluminum Oxide, Al_2O_3, (998 Alumina, McDannel Refractory Procelain Company, Beaver Falls, Pennsylvania, 15010) or of mullite (MV33) from the same source. The test schematic appears below in Figure 4.9. The tube geometrics for both materials are similar with nominal values listed below Figure 4.9, and with eccentricities and standard deviations given in Table 4.1.

Testing Procedures

The general procedure followed was ASTM Standards for rods, 1977, Part 17, pages 104-11.

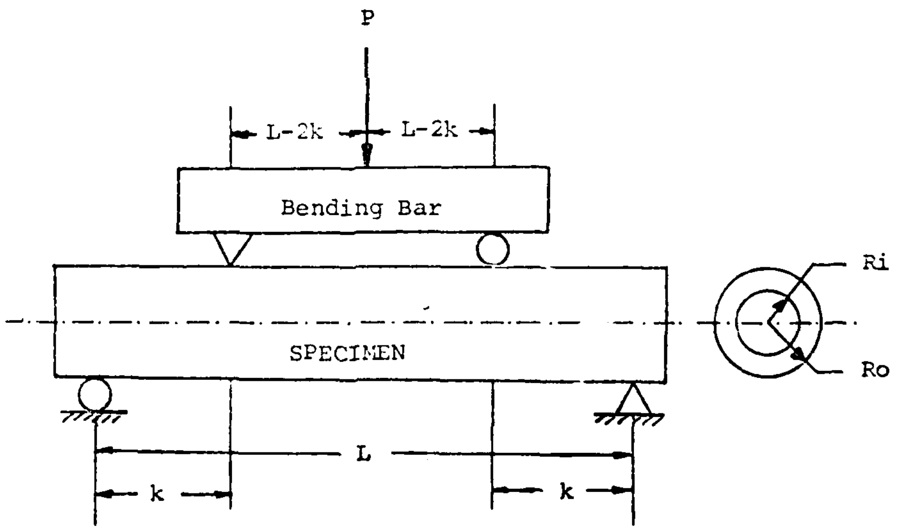

Figure 4.9. Testing Procedure for Bending Specimen

Observations:

Referring to Figure 4.9, general dimensions are in inches:

L	=	10
K	=	3.6
(L-2k)	=	2.8

R_o = .4999 (Alumina)

R_i = .3091 (Alumina)

V_g = .6789 (Alumina) (under tension)

R_o = .5132 (Mullite)

R_i = .3661 (Mullite)

V_g = .5689 (Mullite) (under tension)

	998 Alumina	Mullite (MV33)
Mean and SD of Maximum OD	1.0010 ± .0021	1.0290 ± .0065
Mean and SD of Direction + to Max. OD Direction	.9985 ± .0027	1.0236 ± .0082
Mean and SD of Minimum ID	.6156 ± .0203	.7276 ± .0087
Mean and SD of Direction + to Min. ID Direction	.6209 ± .0234	.7367 ± .0074

Table 4.1. Specimen Means and Standard Deviations in Inches for Inner and Outer Diameters

N = 50 (Alumina)   N = 50 mullite

Analysis of Test Results:

The technique used in the computer program HOLLOW.FOR and DIN.FOR, is an iteration method where the values of Weibull parameters, c, m, and σ_u are found by the minimization of residual errors in the experimentally determined fracture probabilities compared to Eq. 4.10 through 4.12, the probability of fracture $F(\sigma)$ is calculated by repeated applications of Simpson's rule [37] to the integrals until a truncation error condition is satisfied. Residual error as calculated by the least-square method is below:

$$Res(c,m,\sigma_u) = w_i\{F(\tilde{\sigma}) - F(\sigma)\}^2 \qquad (4.13)$$

where $F(\tilde{\sigma}) = \frac{i}{n+1}$ [Mean Rank Method for the experimental fracture loads].

This process perturbs values of c, m, and σ_u until the Eq. 4.13 is minimized. This gives the final values of Weibull parameters for Alumina.

2-Parameter Family	3-Parameter Family
$c = 0.403E-27$ in.$^{2m-3}$lbs.$^{-m}$ .391E-46 M^{2m-3} N^{-m}	$c = 0.403E-27$ in.$^{2m-3}$lbs.$^{-m}$ .391E-46 M^{2m-3} N^{-m}
$m = 6.20$ (dimensionless)	$m = 6.20$ (dimensionless)
$\sigma_u = 0.0$ p.s.i./MPa	$\sigma_u = 0.0$ p.s.i./MPa
$\sigma_o = 26,212$ p.s.i. 180.73 MPa	$\sigma_o = 26,212$ p.s.i. 180.73 MPa
Res = 0.02434	Res = 0.02434

Table 4.2:Weibull Parameters for Alumina 998

The experimental results are given in Table 4.3. This table depicts failure probability estimates via the two- and three-parameter Weibull distributions in comparison to the mean rank experimental results. Table 4.4 depicts those specimens that failed abnormally and were not used for data collection. The residual is minimized with the two parameter family, thus, Table 4.2 entries are identical. Another illustration is given where the Weibull parameters of Table 4.2 are assumed for a one cubic inch specimen under uniaxial stress states. Thus, a one cubic inch specimen exhibits a 50% chance of fracture if stressed uniaxially and uniformly to 24.6 ksi.

Specimen Designation	Fracture Load P* (lbs.)	Moment M PK/2* (lb-in)	Rank i	F(M) i/n+1	Fracture Probability at Failure Moment, M F(M)	
					2-Parameter	3-Parameter
A2	1010	1818	1	0.04762	0.024402	0.024402
A10	1210	2178	2	0.09524	0.074186	0.074186
A22	1365	2457	3	0.14286	0.15019	0.15019
A23	1395	2511	4	0.19047	0.16992	0.16992
A5	1475	2655	5	0.23809	0.23168	0.23168
A4	1510	2718	6	0.28571	0.26273	0.26273
A9	1610	2898	7	0.33333	0.36467	0.36467
A17	1620	2916	8	0.38095	0.37585	0.37585
A21	1730	3114	9	0.42857	0.50773	0.50773
A18	1745	3141	10	0.47619	0.52655	0.52655
A11	1750	3150	11	0.52380	0.53284	0.53284
A1	1785	3213	12	0.57143	0.57705	0.57705
A16	1865	3357	13	0.61905	0.67674	0.67674
A14	1875	3375	14	0.66666	0.68881	0.68881
A25	1885	3393	15	0.71428	0.70076	0.70076
A6	1905	3429	16	0.76190	0.72420	0.72420
A12	1915	3447	17	0.80952	0.7358	0.7358
A3	2005	3609	18	0.85714	0.82948	0.82948
A15	2140	3852	19	0.90476	0.929235	0.929235
A19	2250	4050	20	0.95238	0.97311	0.97311

Table 4.3 Experimental Results for 4-Point Bending Test for A Circular Cross-Section Tube of Alumina 998

* English system used since equipment is calibrated in pounds.

Specimen Designation	Fracture Load (lbs.)	Why Rejected
A7	1770	Failed out of gage length
A8	1690	Testing Machine Failed Then Pulsed Causing Shock
A13	1640	Failed Under Support
A20	1440	Failed Under Support
A24	1595	Failed Under Support

Table 4.4. Experimental Results For Rejected Alumina 998 Bend Test Specimens

Figure 4.10 demonstrates that the Alumina fracture curve is a relatively broad one typical of experiments in which care is taken in the experimental design. Frequently attempts to load brittle specimens in pure tension result in an even broader apparent curve than the one of Figure 4.10 because there are inherent small misalignments in the experimental equipment. These aberrations produce stresses that reconfigure material exhibiting plasticity. Brittle materals are subjected to stresses which only degrade by fracture at a higher level than mean or macroscopic value sensed by the recording equipment. The Weibull modulus is a recognized measure of the combined uniformity of the experimental design and specimen strength predictability. For this material and test, a value of 6.2 is higher than typical.

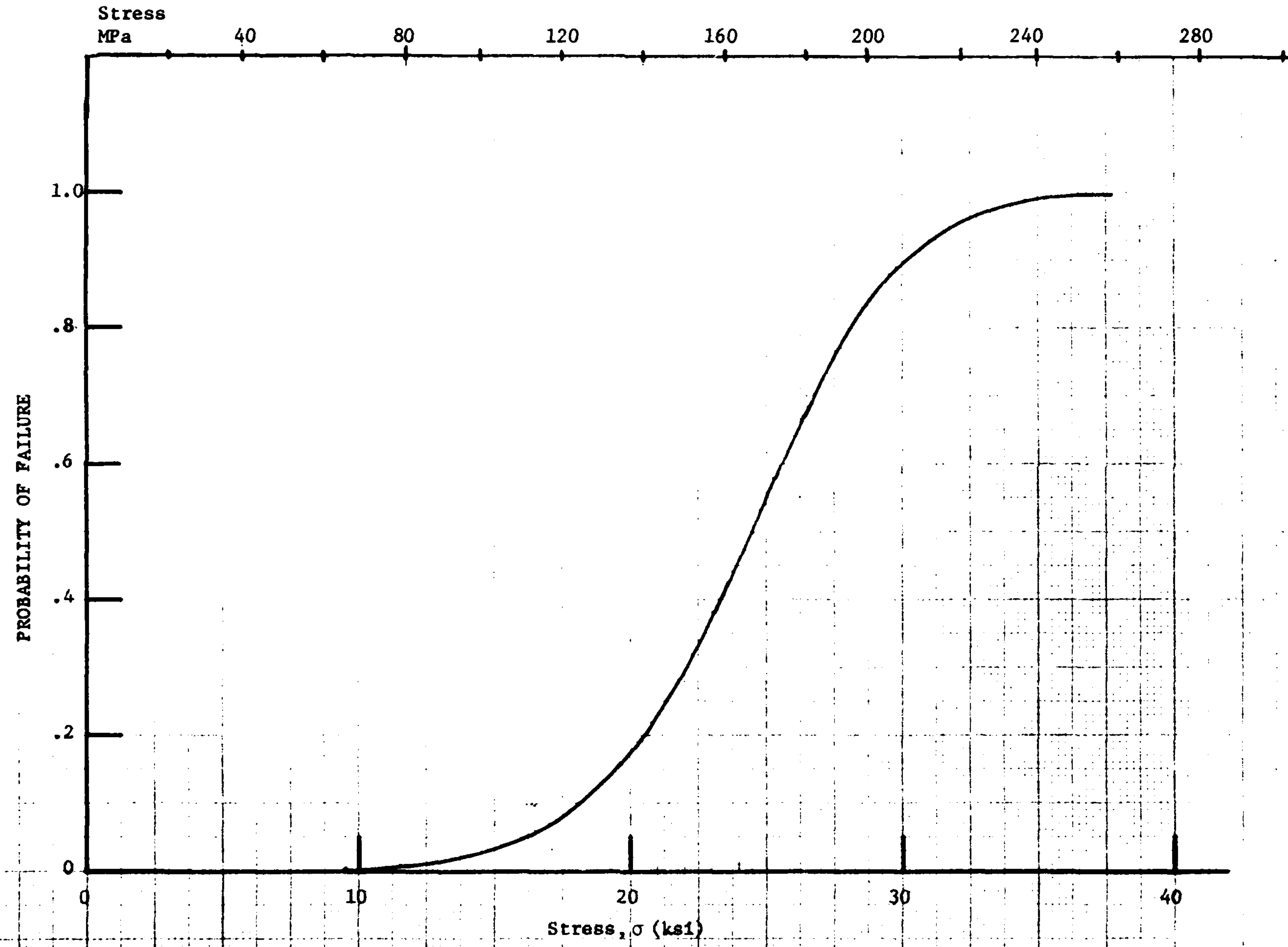

FIGURE 4.10. FAILURE PROBABILITY CURVE FOR A UNIT VOLUME CONSTANT STRESS SPECIMEN OF ALUMINA 998

The results of the mullite bend tests are given in Table 4.5 with Table 4.6 representing the 22 specimens used to determine the parameters of Table 4.5. Table 4.7 is a list of rejected specimens of which only two occurred.

The mean load at failure of the mullite at 843 pounds is significantly below the corresponding load of alumina at 1,702 pounds. It should be noted that even though the mullite is about one-half the strength of alumina, the dispersion to strength ratio of both materials is about the same.

As with alumina, the mullite tests were used to generate Weibull parameter sets to produce the values below:

2-Parameter Family		3-Parameter Family	
c	$= .725E-20\ in.^{2m-3}\ lbs.^{-m}$ ($.6874E-34 M^{2m-3} N^{-m}$)	c	$= .725E-20\ in.^{2m-3} lbs.^{-m}$ ($.6874E-34 M^{2m-3} N^{-m}$)
m	$= 4.90$	m	$= 4.90$
σ_u	= 0.0 p.s.i./M Pa	σ_u	= 0.0 p.s.i./M Pa
σ_0	= 12,887 p.s.i. (88.856 M Pa)	σ_0	= 12,887 p.s.i. (88.856 M Pa)
Res	= .0544	Res	= .0544

Table 4.5: Weibull Parameters for Mullite (MV33)

Once again the two parameter Weibull distribution was found to minimize the results as well as any three-parameter distribution.

Specimen Designation	Fracture Load P* (lbs.)	Moment PK/2* (lb-in)	Rank i	F(M) i/n+1	Fracture Probability Failure Moment, M F(M) 2-Parameter	3-Parameter
M23	530	954	1	0.0526	0.0742	0.0742
M24	550	990	2	0.1053	0.0882	0.0742
M5	595	1071	3	0.1579	0.1270	0.0742
M19	710	1278	4	0.2105	0.2764	0.0742
M21	740	1332	5	0.2632	0.3272	0.0742
M1	770	1386	6	0.3158	0.3824	0.0742
M10	800	1440	7	0.3684	0.4407	0.0742
M9	810	1458	8	0.4211	0.4608	0.0742
M14	825	1485	9	0.4737	0.4912	0.0742
M17	830	1494	10 **	0.5263	0.5014	0.0742
M22	830	1494	10 **	0.5263	0.5014	0.0742
M18	850	1530	11	0.5789	0.5426	0.0742
M2	860	1548	12 **	0.6316	0.5632	0.0742
M4	860	1548	12 **	0.6316	0.5632	0.0742
M8	860	1548	12 **	0.6316	0.5632	0.0742
M13	875	1575	13	0.6842	0.5940	0.0742
M16	970	1746	14	0.7368	0.7756	0.0742
M11	1000	1800	15 **	0.7894	0.8236	0.0742
M12	1000	1800	15 **	0.7894	0.8236	0.0742
M7	1050	1890	16	0.8421	0.8896	0.0742
M6	1100	1980	17	0.8947	0.9372	0.0742
M3	1130	2034	18	0.9474	0.9575	0.9575

* English system used since equipment is calibrated in pounds.

** Multiple entries treated with proportionately higher weights.

Table 4.6: Experimental Results for 4-Point Bending Test for a Circular Cross-Section Tube of Mullite MV33

Specimen Designation	Maximum Load	Remarks
M14	840	Fractured out of gage length
M20	1050	Fractured out of gage length

Table 4.7: Experimental Results for Rejected Mullite MV33 Bend Test Specimens

The graph for the Mullite parameters corresponding to Figure 4.10 for Alumina appear as Figure 4.11. The significatly lower strength of mullite can easily be demonstrated between the two materials when Figures 4.10 and 4.11 are compared.

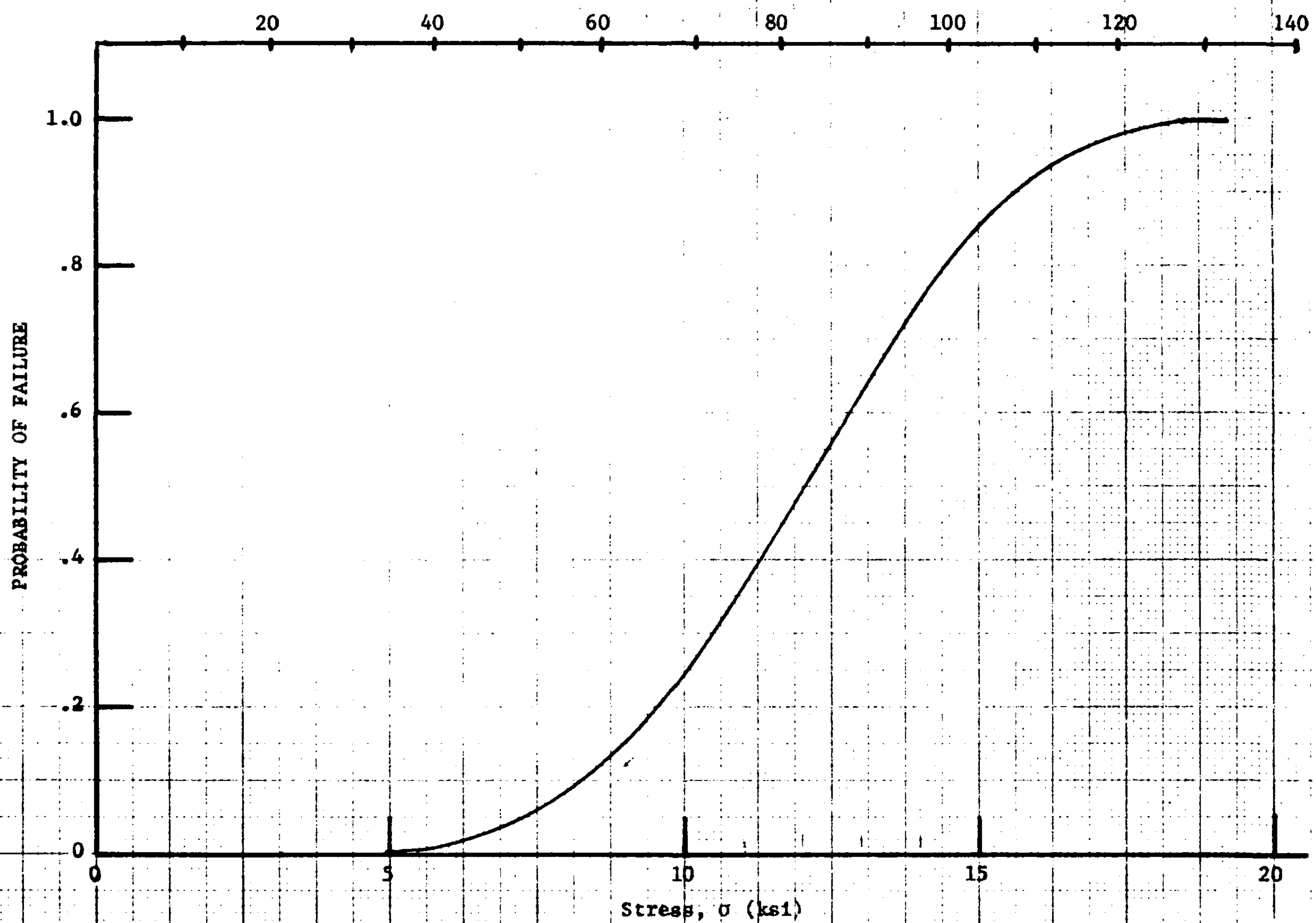

FIGURE 4.11. FAILURE PROBABILITY CURVE FOR A UNIT VOLUME CONSTANT STRESS SPECIMEN OF MULLITE MV33

Examination of Fractured Specimens

Some alumina specimens, Figure 4.12, failed through a single crack wholly within the gage length while no mullite tubes failed wholly in a single crack pattern.

The least complex crack surface of a mullite specimen was compound where 1/2 inch wide sector was separated, Figure 4.13, even then, failure was wholly within the gage length.

The mullite failed in every case with more splintering and chipping than the alumina. Thus, all mullite specimens were taped for safety and retrieval of splinters. While Mullite fractures were more complex, the alumina specimens exhibited the most unpredictable failure geometries; they ranged from the simple fracture of Figure 4.12 to fractures where a variety of compound shapes occurred designated by multiple tension compount fracture (Figure 4.14), multiple compression compound fracture (Figure 4.15), and two section fracture with a compression axial split (Figure 4.16). In no cases, however, did noticeable spalling or chipping of other than material powder occur.

On the other hand, the mullite samples all exhibited a smaller variety of fracture patterns with apparent single fracture initiation locations on the tension side with eminating ray-like cracks toward the compression side similar to Figure 4.15 in the alumina tests. These mullite figures are listed in increasing order of complexity, Figures 4.17, 4.18, and 4.19.

In Figures 4.13 and 4.18, there is clear evidence of mullite spalling in the compression regions. Of course, strain energy densities were highest on the upper and lower regions of the specimens.

While it cannot be seen clearly, many of the alumina specimens have crack bifurcations in regions where there is an abrupt change in crack path. For example, in Figures 4.14 and 4.16 where the 'major' crack path has propagated extensively, the crack has not opened throughout the material. In strong light specimens 4.14 and 4.16 reveal these bifurication points and hidden cracks near the neutral axis plane again where the visible cracks abruptly change direction. No such phenomenon was detected in any of the mullite specimens although they were more opaque.

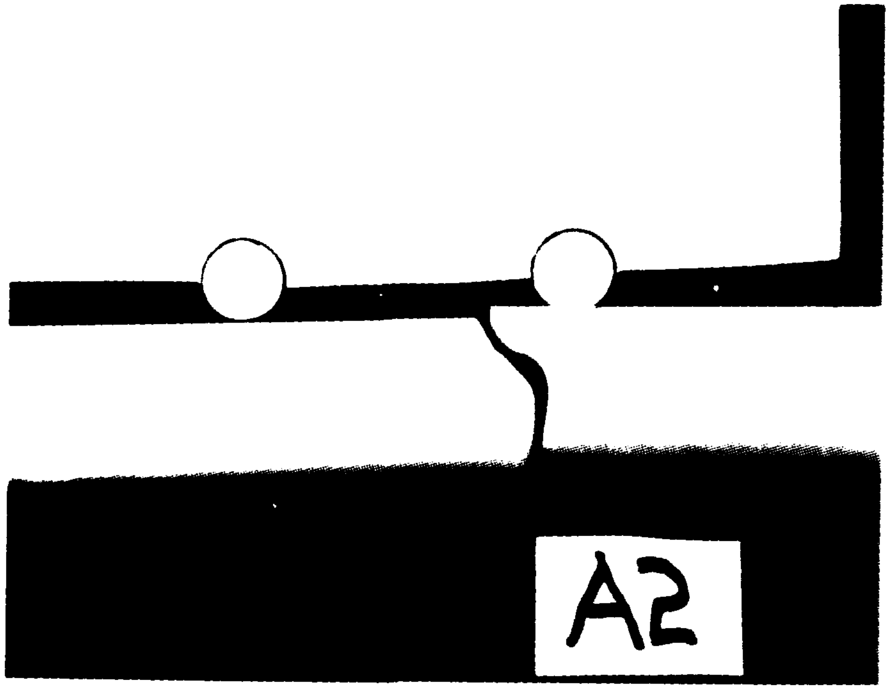

Figure 4.12. Alumina Specimen A2 After Fracture

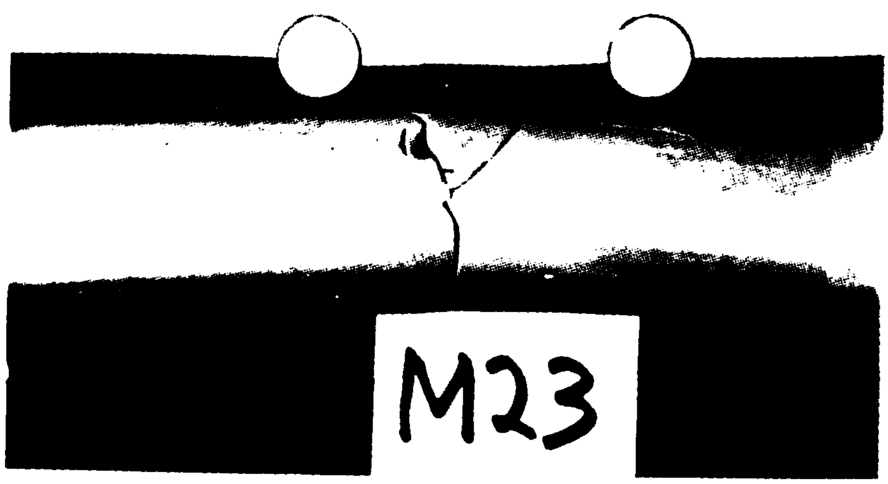

Figure 4.13: Mullite Specimen M23 After Fracture

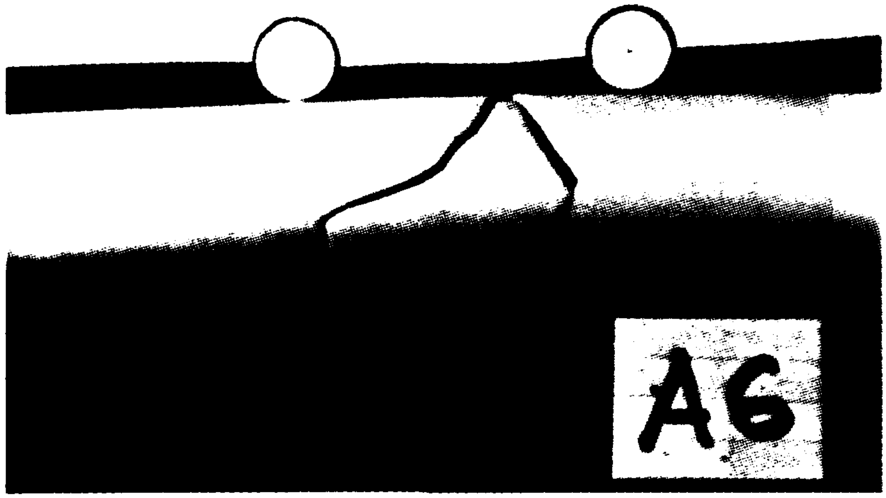

Figure 4.14. Multiple Tension Compound Fracture of Alumina Specimen A6

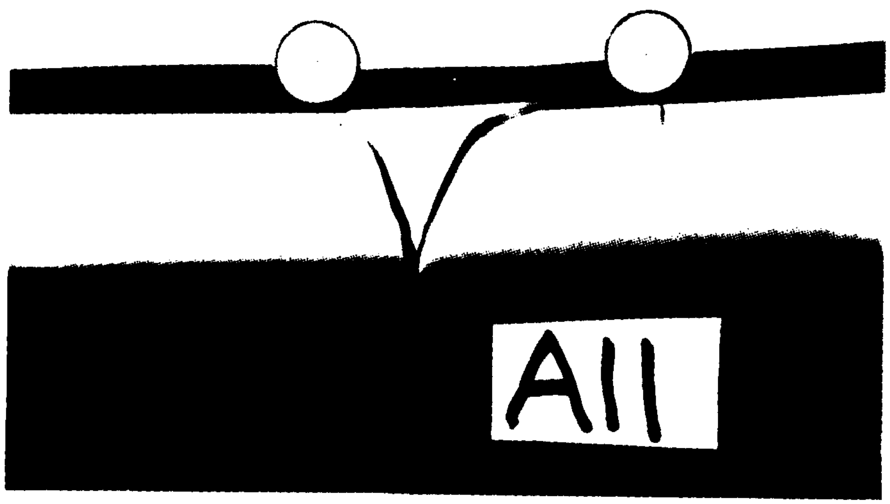

Figure 4.15. Multiple Compression Compound Fracture of Alumina Specimen A11

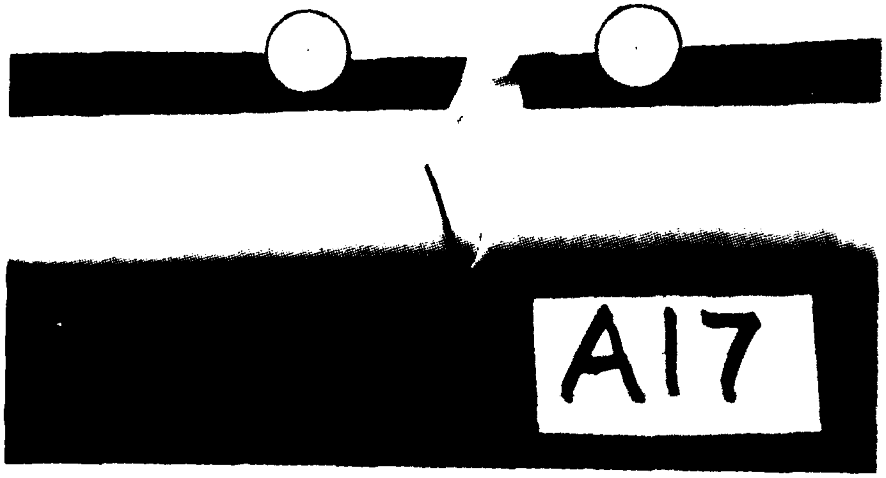

Figure 4.16: Two-Section Fracture with a Compression Axial Split in Alumina Specimen A17

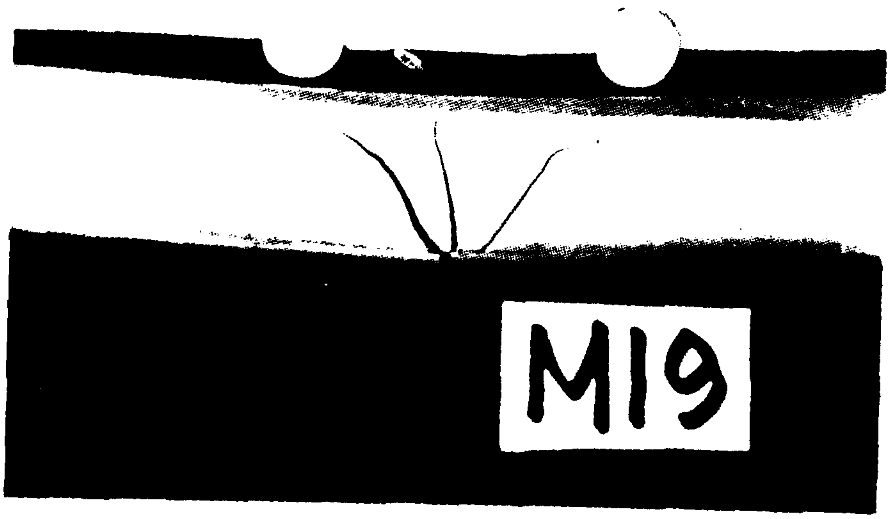

Figure 4.17. Mullite Bend Specimen M19 Multiple Fracture

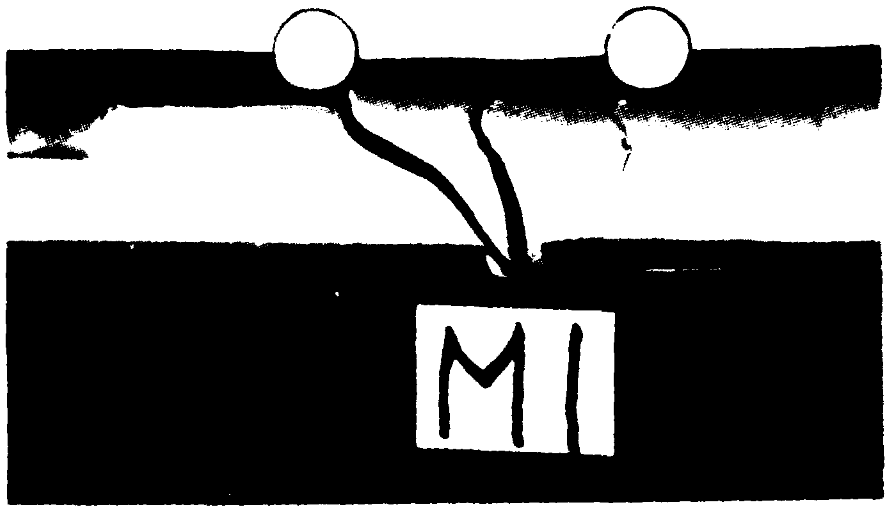

Figure 4.18. Mullite Bend Specimen M1 Multiple Fracture

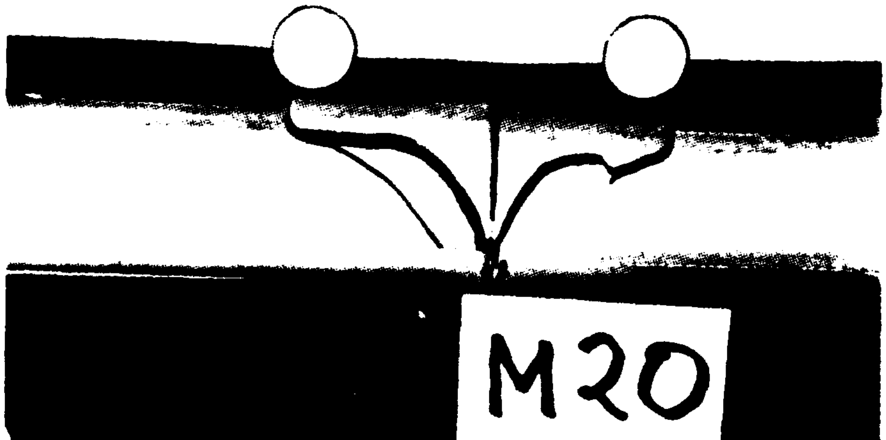

Figure 4.19: Mullite Bend Specimen M20 Multiple Fracture

CONCLUSION

While it was originally expected that a three-parameter Weibull family would be required to describe adequately the probability of fracture in both Alumina and Mullite, it was found that the 2-parameter family produced the same minimum residual sum of squares. As a result, the parameter family was disregarded in favor of the simpler distribution for all bending tests.

The mean failure load of the Alumina tubes was 1702 lbs in four-point loading vs 843 lbs for Mullite. That is equivalent to a stress level of 170 MPa (24.6 ksi) for Alumina and 83.4 MPa (12.1 ksi) for Mullite in a one (1) cu. in. specimen of uniform stress at a 50% chance of failure.

While it is appropriate to employ specimens designed to be operated on precision aligned axial tensil testing equipment, the use of these machines and costly specimens have no advantages over properly designed four-point loading tests. Few specimens demonstrated cracks or crushing near the points of supports.

While the mathematics required in the minimization of residuals for a least square method solution is not closed-form in the case of rods or tubes, the testing simplicity compensates for the minor problem. It is, however, true that the computer model producing the Weibull paramenters could be made to operate more efficiently and automatically.

In order that various hypotheses can be tested in dealing with failure from multiaxial stress states, several stress tensor ratios must be employed. The subsequent or follower contract report N00019-79-PR-RL218, will address parallel work in torsion.

REFERENCES

[1] "Machine Design," A Penton/IPC Publication, March 8, 1979.

[2] William D. Halsey, (Editorial Director), "Collier's Encyclopedia," Vol. 5 of 24 Vols., 1973.

[3] Craft, W. J., "Creation of a Ceramics Handbook," 1974.

[4] Ruoff, Al, "Material Science." Prentice-Hall, Inc., Englewood Cliffs, N.J., 1973.

[5] Berch, C. F., "Properties of Ceramics for Structural and/or High Temperature Use, Need for Control, Measurement and Compilation," Mechanical and Thermal Properties of Ceramics, Proceedings of a Symposium, N.B.S.; Special Publication 303, April, 1968.

[6] Bradt, R.C., et. al., "Fracture Mechanics of Ceramics," Vol. 2, Plenum Press, New York-London, 1973.

[7] Robinson, J. N., Journal of Physics, Scientific Instruments, 5 (2), p. 171, (1972).

[8] Duckworth, W. H., Comment on "Leading Edge Design with Brittle Materials," Antony, F. M., and Mistretta, A. L., "Symposium on Design with Materials that Exhibit Brittle Behaviour," Vol. 1, Materials Advisory Board, National Academy of Sciences Report -- MAB-175-M, p. 285, (1960).

[9] Finlay, Walter L., (Chairman), "Ceramic Processing," Material Advisory Board, National Research Council, Publication 1576, National Academy of Science, 1968.

[10] Dukes, W. H., "Handbook of Brittle Material Design Technology," Advisory Group for Aeronautical Research and Development, Paris, France, October, 1966.

[11] Weibull, W., "The Phenomenon of Rupture in Solids," Ingeniors Vetenskaps Akadamien Handlingar, p. 153, (1939).

[12] Weibull, W., "A Statistical Distribution Function of Wide Applicability," Journal of Applied Mechanics, September, 1951, p. 293-297.

[13] Barnett, R.A., et. al., AFFDL-TR-66-220, March, 1966.

[14] Margetson, J., "Statistical Theory of Brittle Failure for an Anisotropic Structure Subjected to a Multiaxial Stress State," AIAA Paper No. 76-632 in the AIAA/SAE, 12th Propulsion Conference, Palo Alto, California, July, 1976.

[15] Broutman, L. J. and Cornish, R. H., "The Effect of Polyaxial Stress States on Failure Strength of Alumina Ceramics," Journal of American Ceramic Society, 48(10), p. 519-526, (1965).

[16] Broutman, L. J., et. al., "Effects of Combined Stresses on Fracture of Alumina and Graphite," Journal of American Ceramic Society, Vol. 53, #12, December, 1970, (649-654).

[17] Sines, George and Irwin, Georg, "Weakest Link Statistics for Fracture," class notes, Material Science Department, UCLA, CA.

[18] Stanley, P., et. al., "The Unit Strength Concept in the Interpolation of Beam Test Results for Brittle Materials," Proceedings of the Institution of Mechanical Engineers, 1976, Vol. 190.49/76, p. 585-595.

[19] Hudson, J. A. and Fairhurst, Charles, "Tensile Strength, Weibull's Theory and A General Statistical Approach to Rock Failure," p. 901-914.

[20] Appendix 3, "Weibull's Statistical Theory of Strength," WADC, TR 53-50, Pt. 1.

[21] Freudenthal, A. M., Fracture, Vol. II, p. 592-621, Edited by Harold Liebowitz, Academic Press, N. Y., 1969.

[22] Heavens, J. W. and Murgatroyd, P.N., "Analysis of Brittle Fracture Stress Statistics," Journal of American Ceramic Society, September, 1970, p. 503.

[23] Davies, D. G. S., "The Statistical Approach to Engineering Design in Ceramics," Proceedings of British Ceramic Society, #22, June, 1973.

[24] "The Analysis of Brittle Components," Appendix 1 to Chapter 5, Report to the Materials Advisory Board Ad Hoc Committee on Ceramic Processing, WA, D.C.

[25] Gregory and Spruill, "Structural Reliability of Re-Entry Vehicles Using Brittle Materials in the Primary Structure," IAS Aerospace Systems Reliability Symposium, 1962.

[26] Barnett, R. C., et. al., "Utilization of Refractory Non-Metallic Materials in Future Aerospace Vehicles," Flight Dynamics Laboratory, Air Force Systems Command, Contract No. AF33-(615)-1494, September, 1965.

[27] Stanley, P., Fessler, H. and Sivill, A. D., "An Engineer's Approach to the Probability of Brittle Components," Proc. Br. Ceramic Society 22, 453 (1973).

[28] Batdorf, S. B. and Crose, J. G., "A Statistical Theory for the Fracture of Brittle Structures Subjected to Nonuniform Polyaxial Stresses," Journal of Applied Mechanics, p. 41, 459, (1974).

[29] Batdorf, S. B., "A Statistical Theory for Failure of Brittle Materials Under Combined Stresses," AIAA Paper, #73-381.

[30] Batdorf, S. B., "Weibull Statistics for Polyaxial Stress State," Journal of American Ceramic Society, January, 1974.

[31] Evans, A. G., "A General Approach for the Statistical Analysis of Multiaxial Fracture," Journal of American Ceramic Society, July - August, 1978, p. 302-308.

[32] Weil, N. W. and Daniel, I. M., "Analysis of Fracture Probabilities in Nonuniformity Stressed Brittle Materials," Journal of American Ceramic Society, Vol. 47, #6, June, 1964.

[33] Daniel, I. M. and Weil, N. A., "The Influence of Stress Gradient Upon Fracture of Brittle Materials," Journal of American Society of Mechanical Engineers, Paper No. 63-WA-228.

[34] Johnson, C. A. and Prochazka, S., "Investigation of Ceramics for High Temperature Turbine Components," Final Report, Naval Air Systems Command, Contract N62269-76-C-0243.

[35] Davies, D. G. S., "Design in Brittle Materials with Special Reference to Silicon Nitride," Fulmer Research Institution, Report R-275/5, March, 1971.

[36] Platts, D. R. and H. P. Kirchner, "Comparing Tensil and Flexural Strength of a Brittle Material," Journal of Material, 6(1), p. 48-59.

[37] Ralston, Anthony, <u>A First Course in Numerical Analysis</u>, McGraw-Hill Book Company, Incorporated, 1965.

[38] Kapur, K. C. and Laberson, L. R., <u>Reliability in Engineering Design</u>, Chapter II, John Wiley & Sons, N. Y.

[39] Mann, N. R., Fertig, K. W., and Scheuer, E. M., "Tolerance Bounds and a New Goodness-of-Fit Test for Two-Parameter Weibull or Extreme-Valve Distribution," Aerospace Research Laboratories, Wright Patterson Air Force Base, Ohio, ARL 71-0077, May, 1971.

APPENDICES

APPENDIX A

APPENDIX A

RELIABILITY PREDICTIONS BASED ON TEST SPECIMENS

In the circumstances, when it is not practical to investigate the integrity of a component through tests on small models, the reliability predictions can be based on data obtained from test specimens. This method requires the development of an approach, where a combined-fracture stress theory is needed to relate the behavior of a unit volume under a complicated stress state to the behavior of the test specimen under a controlled stress state. Development of such an approach is far from complete; however, based on a series model, Barnett et.al. (26) proposed a simple theory which is often used to predict behavior of a volume subject to a general stress field.

If σ_1, σ_2, and σ_3 are principal stresses acting on a uniformly stressed unit volume V_{un}, the reliability of the volume is:

$$1 - F(\sigma) = \left[1 - F(\sigma_1)\right] \left[1 - F(\sigma_2)\right] \left[1 - F(\sigma_3)\right] \qquad \text{(A.1)}$$

where;

$1 - F(\sigma)$ = reliability of the volume

$F(\sigma)$ = The fracture probability of a unit volume under a pure tensile stress σ

Eq. (1.1) can be used for any uniformly stressed basic unit for which $F(\sigma)$ has been established, including, for example, infinitesimal volumes. It is however an assumption of independence of effect due to the stress tensor components actions.

The simplest way to determine the reliability-strength trade-off is to test full-scale prototypes, where neither a stress nor strength

analysis is required, but the drawback is expense. The testing of scale models costs less and still avoids the need for stress analysis. However this technique requires a knowledge of strength-volume relationship. Since neither of these approaches provides much basic information about the material being tested, therefore subsequent designs with the same material must be developed from scratch.

The most sophisticated approach - the statistical theory of which is explained above - requires not only data from test specimen requires a detailed stress analysis. Small, relatively inexpensive specimens are tested to determine the reliability characteristics of small volumes which further leads to predict prototype behavior. The entire analysis requires six steps.

1. Obtain the tensile-strength distribution $F_{V_g}(\sigma)$ using a tension specimen with gage volume V_g.
2. Perform a complete stress analysis of the component.
3. Divide the component into n convenient volumes, $V_1, V_2, \ldots\ldots, V_n$. Each volume should be sufficiently small so that it contains approximately a constant stress state.
4. Determine the 'worst' stress condition in each volume V_j and assume that the corrosponding principal stresses σ_1, σ_2, and σ_3 act uniformly throughout the volume.
5. Determine the reliability of each volume $(1-F_V)_j$ by first finding the reliability of the gage volume under the principal stresses through the application of Eq. (1.1);

$$[1-F_{V_g}(\sigma_1,\sigma_2,\sigma_3)] = [1-F_{V_g}(\sigma_1)]\ [1-F_{V_g}(\sigma_2)]\ [1-F_{V_g}(\sigma_3)] \tag{A.2}$$

Then scale gage-volume reliability to find $(1-F_V)$ by using the Eq. (1.3)*.

$$(1-F_V)_j = (1-F_{V_g})^{V_j/V_g} \qquad \text{(A.3)}$$

6. Use Eq. (1.4) which is based on weakest-link hypothesis, to establish the reliability of the entire structure, $(1-F(\sigma)$ from the reliability of the volumes V_j.

$$1-F(\sigma) = (1-F_1)(1-F_2)\ldots\ldots.(1-F_n) = \sum_{j=1}^{n}(1-F_j) \qquad \text{(A.4)}$$

$$1-F(\sigma) = \sum_{j=1}^{n}(1-F_V)_j \qquad \text{(A.5)}$$

---

* Eq. (1.3) is based on the extreme value statistics, which furnish with an important necessary condition for a series material that does not require the specific form of the distribution function nor a knowledge of the combined-stress theory appropriate for the material. Specifically, when the loading and geometry of two different size components are similar, their distribution function $F(\sigma)$ must scale according to the following relationship when the material obeys the series model.

$$1 - F_2(\sigma_2) = 1 - F_1(\sigma_1)^{V_2/V_1}$$

where F_i is the fracture probability of the i^{th} structure, V_i is the volume of the i^{th} structure.

APPENDIX B

APPENDIX B

Newton-Raphson Iteration Method for Matrix Equations of Weibull Parameters

The residue equation is:

$$R(c,m,\sigma_u) = \sum_{i=1}^{n} w_i \left[\tilde{F}_i - \left\{1 - \exp\{-c(\sigma - \sigma_u)^m\}\right\}\right]^2 \quad \text{(B.1)}$$

where R = Residue as function c, m, and σ_u

$\tilde{F}_i$ = Data Points

Simplification of Eq. (2.1) takes the form of:

$$R = -2 \quad \Sigma\, w_i \left\{ \approx{F}_i e^{-u_i} + e^{-2u_i} + \approx{F}_i^{\,2} \right\} \quad \text{(B.2)}$$

where $\approx{F}_i = (1 - \tilde{F}_i)$

$u_i = c(\sigma_i - \sigma_u)^m$

Minimization of residue R, requires that partial derivatives of Eq. (2.9) with respect to c, m, and σ_u be zero.

$$\frac{\delta R}{\delta c} = 2 \sum_{i=1}^{n} w_i \left\{ F_i e^{-u_i} - e^{-2u_i} \right\} (\sigma_i - \sigma_u) \quad \text{(B.3)}$$

$$\frac{\delta R}{\delta m} = 2 \sum_{i=1}^{n} w_i \left\{ \approx{F}_i e^{-u_i} - e^{-2u_i} \right\} c\, \ell n(\sigma_i - \sigma_u)(\sigma_i - \sigma_u)^m \quad \text{(B.4)}$$

$$\frac{\delta R}{\delta \sigma_u} = -2 \sum_{i=1}^{n} w_i \left\{ \approx{F}_i e^{-u_i} - e^{-2u_i} \right\} c\, m\, (\sigma_i - \sigma_u)^{m-1} \quad \text{(B.5)}$$

Again, a Newton-Raphson solution of c, m, and σ_u requires that the partial derivatives of Eqs. (B.3), (B.4), and (B.5) with respect to c, m, and σ_u should be satisfied. The following is the desired matrix expressed in a symbolic form.

$$\begin{bmatrix} R,c \\ \\ R,m \\ \\ R,\sigma_u \end{bmatrix} = - \begin{bmatrix} R,cc & R,cm & R,c\sigma_u \\ & & \\ & R,mm & R,m\sigma_u \\ \text{Symmetric} & & \\ & & R,\sigma_u\,\sigma_u \end{bmatrix} \begin{bmatrix} \delta c \\ \\ \delta m \\ \\ \delta\sigma_u \end{bmatrix} \tag{B.6}$$

where in condensed form

$$u_i = c(\sigma_i - \sigma_u)^m$$

$$R,_{v_j} = 2\,\Sigma\, w_i \left\{ \tilde{\tilde{F}}_i e^{-u_i} - e^{-2u_i} \right\} \frac{\delta u_i}{\delta v_j}$$

$$R,_{v_j v_k} = 2\,\Sigma\, w_i \left\{ \tilde{\tilde{F}}_i e^{-u_i} - e^{-2u_i} \right\} \frac{\delta u_i}{\delta v_j \delta v_k} +$$

$$\Sigma\; w_i \left\{ 2e^{-2u_i} - \tilde{\tilde{F}}_i e^{-u_i} \right\} \frac{\delta u_i}{\delta v_j} \frac{\delta u_i}{\delta v_k} \qquad \text{(B.7)}$$

v_j = one of $\{c, m, \sigma_u\}$, j = 1, 2, 3.

Solution of this matrix gives the corrections c, m, and σ_u to initial guesses of c, m, and σ_u. Refined values of Weibull parameters are obtained by adding these correction values to the initial guesses and repeating until the values converge (computer program NEWTON.FOR).

Unfortunately, this method is highly unstable and frequently only converges if the initial values are within ± 5% of the correct values. The problem, therefore, is to produce very accurate initial guesses easily or abandon this technique as a less useful one. One mechanism albeit not entirely successful of selecting initial values is listed below;

<u>Initial Prediction and Stepping Method</u>

In this method a set of three points σ_A, σ_B, and σ_C is chosen for the analysis of Weibull parameters. We let

$$\sigma_A = \sigma\left(\frac{n}{4}\right), \quad \sigma_B = \sigma\left(\frac{n}{2}\right), \quad \sigma_C = \sigma\left(\frac{3n}{4}\right) \tag{B.8}$$

where n is a multiple of 4.

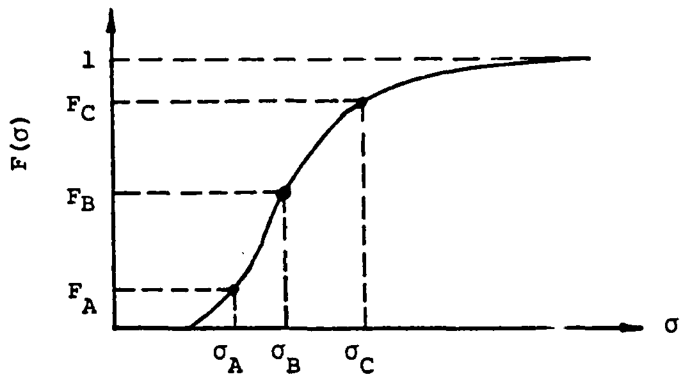

Figure B.1. Selection of Three Data Points

This leads to a technically simple approximation for c, m, and σ_u. Expressing the Weibull distribution for point σ_A , we obtain

$$F_A = 1 - \exp\left\{-c(\sigma_A - \sigma_u)^m\right\} \tag{B.9}$$

and similar expressions for points σ_B, and σ_C.

Taking $\ell n\ \ell n$ we have:

$$\ell n\ c + m\ \ell n(\sigma_A - \sigma_u) = K_A \tag{B.10}$$

similarly for points σ_B, and σ_C we have:

$$\ell n\ c + m\ \ell n(\sigma_B - \sigma_u) = K_B \tag{B.11}$$

$$\ell n\ c + m\ \ell n(\sigma_C - \sigma_u) = K_C \tag{B.12}$$

where

$$K_A = \ell n \ell n \left(\frac{1}{1 - F_A} \right) \qquad \text{and similarly for } K_B \text{ and } K_C.$$

Simplification of Eqs. (2.10), (2.11), and (2.12) gives:

$$m \, \ell n \left(\frac{\sigma_A - \sigma_u}{\sigma_B - \sigma_u} \right) = K_A - K_B \tag{B.13}$$

$$m \, \ell n \left(\frac{\sigma_B - \sigma_u}{\sigma_C - \sigma_u} \right) = K_B - K_C \tag{B.14}$$

by eliminating m we obtain:

$$F(\sigma_u) = \gamma \, \ell n \left(\frac{\sigma_u - \sigma_A}{\sigma_u - \sigma_B} \right) + \ell n \left(\frac{\sigma_u - \sigma_C}{\sigma_u - \sigma_B} \right) \tag{B.15}$$

where

$$\gamma = \frac{K_B - K_C}{K_A - K_B}$$

Thus the problem is reduced to finding σ_u of Eq. (B.15). The Newton-Raphson iteration method for the solution of parameter σ_u requires;

$$\sigma_{u_n} = \sigma_{u_o} - \frac{F(\sigma_u)}{F'(\sigma_u)} \tag{B.16}$$

where

σ_{u_n} = New value of σ_u after each iteration

σ_{u_o} = Preceding value of σ_u used for reiteration

$F'(\sigma_u)$ = First derivative of $F(\sigma_u)$

Expansion of Eq. (2.16) takes the form of:

$$\sigma_{u_n} = \sigma_{u_o} - \frac{\gamma \ln \left\{ \dfrac{\sigma_{u_o} - \sigma_A}{\sigma_{u_o} - \sigma_B} \right\} + \ln \left\{ \dfrac{\sigma_{u_o} - \sigma_C}{\sigma_{u_o} - \sigma_B} \right\}}{\left\{ \dfrac{1}{\sigma_{u_o} - \sigma_B} \right\} \left[\gamma \left\{ \dfrac{\sigma_A - \sigma_B}{\sigma_{u_o} - \sigma_A} \right\} + \left\{ \dfrac{\sigma_C - \sigma_B}{\sigma_{u_o} - \sigma_C} \right\} \right]} \tag{B.17}$$

solution of the above expression gives the value of σ_u by iteration. Once σ_u is determined, the values of c and m can be found from Eqs. (B.10) and (B.13).

Unfortunately, it can be shown that solution of Eq. (B.17) can lead to σ_u which generates complex c and m even for $\sigma = \sigma_A$, σ_B, or σ_C, if real probabilities are generated. When real c and m are found, it is still often that the Newton-Raphson process does not converge, further improvement in solution technique is needed. The iterative technique is included as a computer program in Appendix E, program 5, NEWTON.FOR.

σ_{u_o} = Preceding value of σ_u used for reiteration

$F'(\sigma_u)$ = First derivative of $F(\sigma_u)$

Expansion of Eq. (2.16) takes the form of:

$$\sigma_{u_n} = \sigma_{u_o} - \frac{\gamma \ln \left\{ \dfrac{\sigma_{u_o} - \sigma_A}{\sigma_{u_o} - \sigma_B} \right\} + \ln \left\{ \dfrac{\sigma_{u_o} - \sigma_C}{\sigma_{u_o} - \sigma_B} \right\}}{\left\{ \dfrac{1}{\sigma_{u_o} - \sigma_B} \right\} \left[\gamma \left\{ \dfrac{\sigma_A - \sigma_B}{\sigma_{u_o} - \sigma_A} \right\} + \left\{ \dfrac{\sigma_C - \sigma_B}{\sigma_{u_o} - \sigma_C} \right\} \right]} \tag{B.17}$$

solution of the above expression gives the value of σ_u by iteration. Once σ_u is determined, the values of c and m can be found from Eqs. (B.10) and (B.13).

Unfortunately, it can be shown that solution of Eq. (B.17) can lead to σ_u which generates complex c and m even for $\sigma = \sigma_A$, σ_B, or σ_C, if real probabilities are generated. When real c and m are found, it is still often that the Newton-Raphson process does not converge, further improvement in solution technique is needed. The iterative technique is included as a computer program in Appendix E, program 5, NEWTON.FOR.

APPENDIX C

APPENDIX C

The Histogram Method for the Solution of Weibull Parameters

Three-parameter Weibull distribution is expressed as:

$$F(\sigma) = 1 - \exp\left\{-c(\sigma - \sigma_u)^m\right\} \tag{C.1}$$

The function $F(\sigma)$ can be determined in several ways. In the mean rank method n tests are conducted and the data is ordered by increasing fracture stress. This yields a sequence of numbers for $\sigma_1 < \ldots\ldots < \sigma_i < \sigma_n$. The estimation of cumulative distribution function, $F(\tilde{\sigma})$, is then given by

$$F(\tilde{\sigma}_i) = \frac{i}{n+1} \quad ; \quad \text{also} \quad F(\tilde{\sigma}_i) = \tilde{F}_i \tag{C.2}$$

A more sophisticated statistical treatment [38] known as the Median Rank method uses the estimator

$$\tilde{F}_i = \frac{i - .03}{n + .04} \tag{C.3}$$

This formula is an approximation to Median Rank values from the imcomplete Beta function.

Other techniques exist which also seek to convert a set of data, i.e., a number of specimens with a number of fraction values to a probability of fracture table. Basically this involves the integration of a histogram, Figure C.1,or frequency distribution $P(\sigma)$, to obtain the

probability of failure curve.

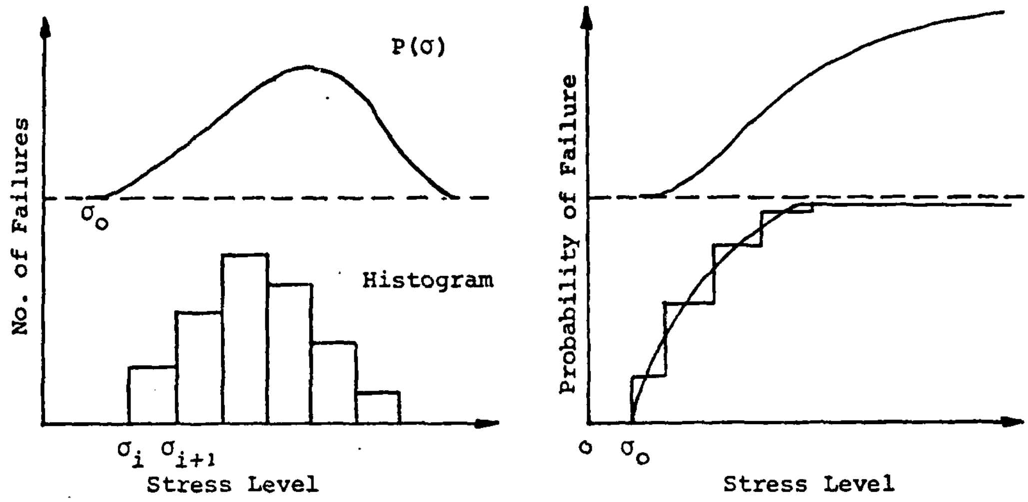

Figure C.1. Probability Distribution

Thus P(in the range σ_i to σ_{i+1})

$$P\left(\frac{\sigma_i + \sigma_{i+1}}{2}\right) = \frac{\text{The Number of failures in the range } \sigma_i \text{ to } \sigma_{i+1}}{n}$$

And once $P(\sigma)$ is known,

$$F(\tilde{\sigma}) = \int_{-\infty}^{\sigma} P(\sigma)\ d\sigma = \int_{\sigma_o}^{\sigma} P(\sigma)\ d\sigma \qquad (C.4)$$

Numerous techniques exist to convert this histogram information to a probability of failure curve, it is assumed then that $F(\tilde{\sigma})$ will be known for a variety of data points, σ so that a table may be devised for σ versus $\tilde{F}$. Thus, it is required that values of the distribution constants be determined for the $F(\sigma)$ curve.

A typical example below, Table C-1, shows how to obtain a

failure probability curve from the discrete element (histogram) approach.

Stress	Rank	Probability of Failure $F(\tilde{\sigma})$		
σ_i	i	$F(\tilde{\sigma}_i)$ vs σ_i		
10.02	1	0	0	$0 \leq \sigma < 10.02$
12.30	2	1/12	0.083	$10.02 \leq \sigma < 12.30$
14.76	3	2/12	0.166	$12.30 \leq \sigma < 14.76$
15.30	4	3/12	0.250	$14.76 \leq \sigma < 15.30$
16.24	5	4/12	0.333	$15.30 \leq \sigma < 16.24$
16.94	6	5/12	0.416	$16.24 \leq \sigma < 16.94$
17.20	7	6/12	0.500	$16.94 \leq \sigma < 17.20$
17.82	8	7/12	0.583	$17.20 \leq \sigma < 17.82$
18.40	9	8/12	0.666	$17.82 \leq \sigma < 18.40$
19.60	10	9/12	0.750	$18.40 \leq \sigma < 19.60$
20.15	11	10/12	0.833	$19.60 \leq \sigma < 20.15$
22.40	12	11/12	0.916	$20.15 \leq \sigma < 22.40$

Table C-1. Stress Level vs Probability of Failure

The histogram and the cumulative distribution function of the data presented in Table C-1 is displayed as follows:

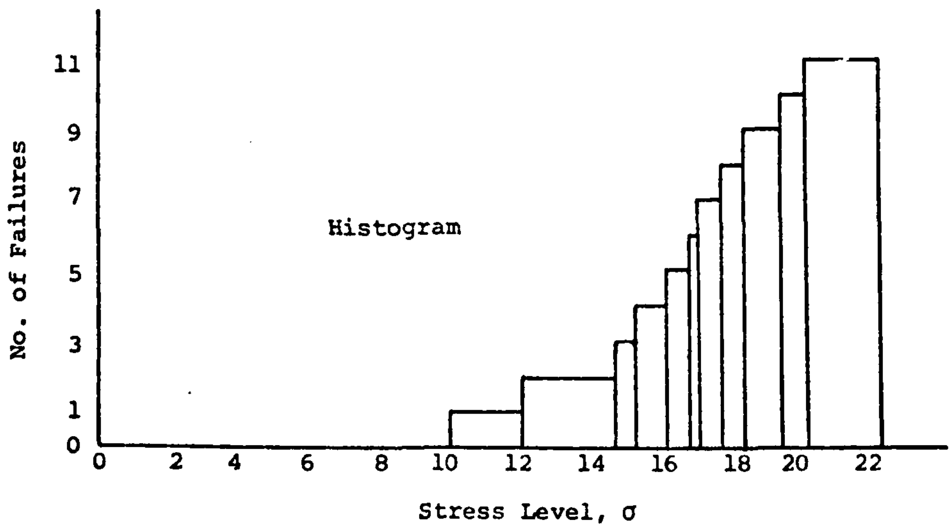

Figure C.2. Cumulative Frequency Distribution of Table C.1 data

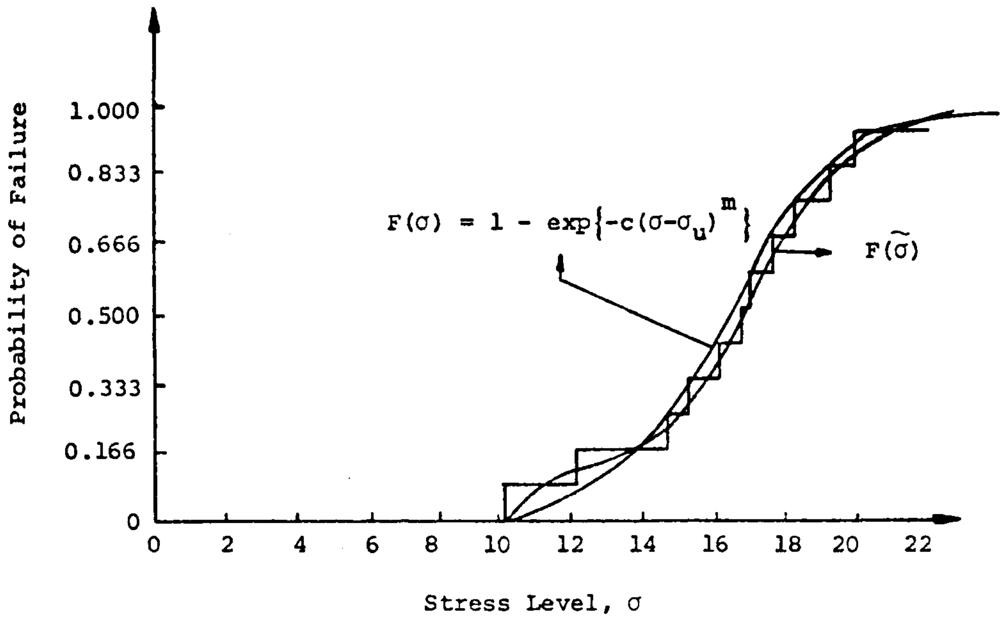

Figure C.3. Probability of Failure for the data of Table C-1.

According to least-square analysis the residue equation expressing the sum of the square of differences between data and predictive equation must be minimized. The residue equation with weights where the cumulative integrated distribution is assumed, Eq. (C.4) is given by:

$$Res(c,m,\sigma_u) = \int_{10.02}^{22.40} \tilde{w}(\sigma) \left\{F(\tilde{\sigma}) - F(\sigma)\right\}^2 d\sigma \qquad (C.5)$$

where $\tilde{w}(\sigma)$ = weight per unit stress.

Expansion of Eq. (3.5) takes the form:

$$Res(c,m,\sigma_u) = \left\{ \int_{10.02}^{12.30} \tilde{w}(\sigma)\{\tfrac{1}{12} - F(\sigma)\}^2 \, d\sigma + \right.$$

$$\int_{12.30}^{14.76} \tilde{w}(\sigma)\{\tfrac{2}{12} - F(\sigma)\}^2 \, d\sigma + \cdots\cdots + \int_{20.15}^{22.40} \tilde{w}(\sigma)\{\tfrac{11}{12} - F(\sigma)\}^2 \, d\sigma \Bigg\} \quad (C.6)$$

or in summation form:

$$\mathrm{Res}(c,m,\sigma_u) = \sum_{i=1}^{n-1} w(\sigma_i) \left\{ F(\tilde{\sigma_i}) - F(\sigma_i) \right\}^2 d\sigma \quad (C.7)$$

where $w(\sigma)$ is assumed constant in each range expressed in Table C-1.

The solution of Eq. (C.7) determines the values of three Weibull parameters c, m, and σ_u. However this method is very cumbersome and sometimes the predictive equation for $F(\sigma)$ is not of closed form as is the case of 4-point bending hollow tube.

APPENDIX D

APPENDIX D

Statistical Properties of Weibull Distribution

The three-parameter Weibull distribution in its cumulative form is given as

$$F(\sigma) = 1 - \exp - \left(\frac{\sigma - \sigma_u}{\sigma_o}\right)^m \tag{D.1}$$

For the case $\sigma_u = 0$, the Eq. (4.1) takes the form of two-parameter Weibull distribution given as:

$$F(\sigma) = 1 - \exp - \left(\frac{\sigma}{\sigma_o}\right)^m \tag{D.2}$$

In this case the fracture can take place at any positive value of the fracture stress.

Since the three-parameter distribution can always be converted to the two-parameter distribution by a simple linear transformation, the two-parameter Weibull distribution is used to illustrate the properties of the Weibull distribution.

The probability density function (p.d.f.) is obtained by differentiating the Eq. (D.2).

$$P(\sigma) = \frac{m}{\sigma_o}\left(\frac{\sigma}{\sigma_o}\right) \exp -\left(\frac{\sigma}{\sigma_o}\right)^m \tag{D.3}$$

taking scale parameter, $\sigma_o = 1$, the Eq. (4.3) can be written as:

$$P(\sigma) = m(\sigma)^{m-1} \exp(-(\sigma)^m) \tag{D.4}$$

A graphical plot of the Eq. (D.4) for different values of shape parameter, m, to show the various forms of the probability

density function has been shown in Figure D-1.

The scale parameter σ_o is used to locate the Weibull distribution along the σ axis. Assuming $\sigma = \sigma_o$ into the cumulative distribution function, Eq. (D.2), it can be easily shown that for any Weibull distribution the probability of failure prior to σ_o is equal to 63.2% and independence of the shape parameter, m.

$$F(\sigma=\sigma_o) = 1 - \exp -\left(\frac{\sigma_o}{\sigma_o}\right)^m$$

$$= 1 - \exp(-1)^m$$

$$= 0.632$$

From the above fact it is quite clear that the scale parameter, σ_o will always divide the area under the p.d.f. into 63.2% for all values of m.

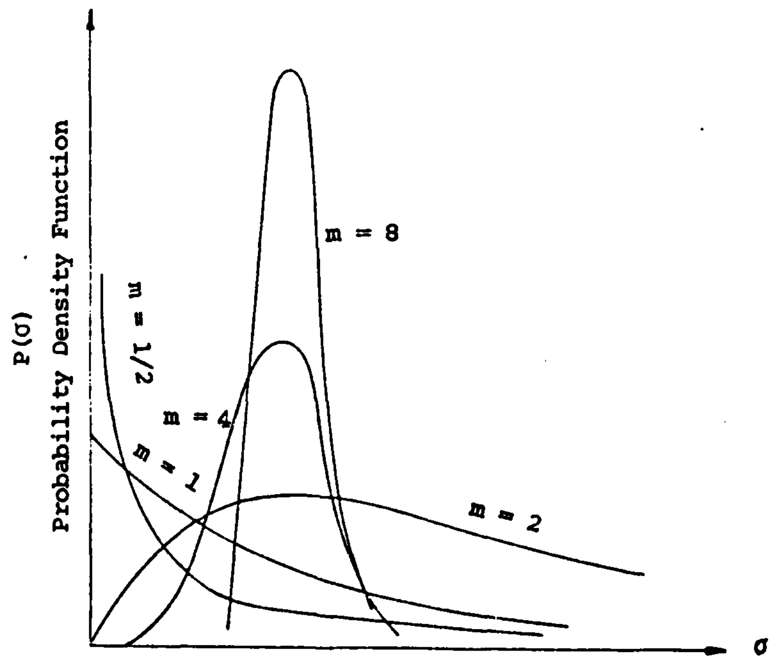

Figure D.1. The Weibull Distribution for Different Values of m

A Goodness-of-Fit Test for the Weibull Distribution

When dealing with Weibull subjected experimental data one often faces a question as to whether the data fits the two-parameter or three-parameter Weibull distribution. The simplest technique one can think of, is to transfer the two-parameter Weibull distribution into a linear relationship by taking the log twice and plotting the data on a graph paper. If the resulting shape of Weibull plot is a straight line then one can easily decide that the data follows a two-parameter Weibull distribution. Failure to get a straight line plot, and especially when the plot curves downwards at the lower end, gives the indication that the experimental data follow a three-parameter Weibull distribution. In this case the value of the threshold stress σ_u must be calculated to get a straight line plot.

Mann et.al. [39] developed a goodness-of-fit test especially for the Weibull distribution which is expected to be more powerful than any of the general goodness-of-fit tests.

The null hypothesis in this case is that the experimental data is two-parameter Weibull distribution. If the null hypothesis is rejected, then other distributions including the three-parameter Weibull distribution, should be considered. The mathematics of the goodness-of-fit test is quite simple and is given as follows:

Let $\sigma_1, \sigma_2, \ldots\ldots, \sigma_r$ represents the first r ordered failure stresses resulting from placing n specimen on test and truncating the test at the time of r^{th} failure $(r \leq n)$.

Defining EK_i as $EK_i = \ell n(\sigma_i)$ for $i=1,2,\ldots\ldots,r.$, the test statistics is given as:

$$S = \frac{\sum_{i=(r/2)+1}^{r-1} \left[\frac{(EK_{i+1} - EK_i)}{M_i} \right]}{\sum_{i=1}^{r-1} \left[\frac{(EK_{i+1} - EK_i)}{M_i} \right]} \tag{D.5}$$

where $(r/2)$ denotes the greatest integer $r/2$; for example, if $r = 9$, then $(r/2) = 4$. The value for M_i's are found in [38], along with the critical value for S.

APPENDIX E

UNIAX.FOR

```
C THIS PROGRAM IS FOR THE UNIAXIAL CONSTANT STRESS FIELDS
C PROGRAM WEIBUL THREE PARAMETERS
C* THE PARAMETERS ARE C, M, AND SIGU
C THIS PROGRAM COMPUTES ALL PARAMETERS BY
C LINEAR REGRESSION METHOD. FOR NOTATION SIGU=SIGO
C THIS PROGRAM HAS BEEN EXECUTED ON DEC-1060 SYSTEM
        DIMENSION X(20),F(20),W(20),EK(20),P(20),WN(20),WM(20)
        WRITE(5,10)
10      FORMAT(1X,'ENTER DATA FILE NO.')
        READ(5,*) ND
        READ(ND,*) N
C ND=NUMBER OF DATA FILE
C N=NUMBER OF WEIBUL POINT PAIRS
C W=ARBITRARY WEIGHTS
  X=FRACTURE STRESS VALUES
        READ(ND,*)  ((X(I),F(I),W(I)),I=1,N)
        DO 1 I=1,N
1       WRITE(5,20) (I,X(I),F(I),W(I))
20      FORMAT(1X,'X(I),F(I),W(I) FORI=',I2,3(1X,E12.6))
        DO 2 I=1,N
        EK(I)=ALOG(ALOG(1./(1.-F(I))))
2       CONTINUE
        NN=5
        JK=0
        INT=10
        RESO=1.E+30
        BEG=-.99*X(1)
        EMD=.99*X(1)
98      H=(EMD-BEG)/FLOAT(INT)
        DO 95 I=0,INT
        SIK=BEG+FLOAT(I)*H
        DO 96 II=1,N
96      P(II)=ALOG(X(II)-SIK)
        CALL LIN(W,WN,P,EK,N,SIK,A,B,RES)
        IF(RES.GT.RESO) GO TO 95
        RESO=RES
        SIGU=SIK
        AG=A
        BG=B
        J=I
95      CONTINUE
        WRITE(5,80) AG,BG,RESO,SIGU,SIGO
C REDIFINE EMD AND BEG AND CONTINUE
        IF (JK.GT.NN) GO TO 97
        JK=JK+1
        IF (J.EQ.0) J=1
        IF (J.EQ.INT) J=INT-1
        EMD=BEG+FLOAT(J+1)*H
        BEG=EMD-2.*H
        RESO=RES
        SIGO=SIGU
        GO TO 98
```

```
80      FORMAT(2X,°AG=°,E12.6,7X,°BG=°,E12.6/,2X,°RESO=°,E12.6,
     1  5X,°SIGU=°,E12.6,5X,°SIGO=°,E12.6)
C EC,ESIGO, AND EM ARE THREE WEIBULL PARAMETERS
97      EC=EXP(AG)
        ESIGO=SIGU
        EM=BG
        VOL=1
C* VOL SHOULD BE CHANGED AS PER PROBLEM
        VOLUN=1
        SIGO=(1./(VOLUN*EC))**(1/EM)
        WRITE(5,100)EC,EM,SIGU,SIGO
100     FORMAT(/,20X,°WEIBUL PARAMETERS ARE°,//,2X,
     1  °EC=°,E12.6,5X,°EM=°,F8.2,5X,°SIGU=°,E12.6,5X,°SIGO=°,E12.5,/)
C CALCULATED PROBABILITIES ARE LISTED AS BELOW
        DO 130 II=1,N
130     P(II)=ALOG(X(II)-SIGU)
        CALL LIN(W,WM,P,EK,N,SIGU,A,B,RES)
        DO 108 I=1,N
        PCAL=1.-EXP(-(VOL/VOLUN)*((X(I)-ESIGO)/SIGO)**EM)
108     WRITE(5,110) PCAL,F(I),W(I)
110     FORMAT(1X,°PCAL,F(I),W(I)=°,E12.6,2(1X,E12.6))
        STOP
        END
C SUBROUTINE LIN CALCULATES VALUES OF CONSTANTS A AND B
        SUBROUTINE LIN(W,WN,P,EK,N,SIGU,A,B,RES)
        DIMENSION  W(20),P(20),EK(20),WN(20)
        C=0.
        D=0.
        E=0.
        G=0.
        H=0.
        DO 4 I=1,N
        C=C+(W(I))
        D=D+(W(I)*P(I))
        E=E+(W(I)*P(I)*P(I))
        G=G+(W(I)*EK(I))
        H=H+(W(I)*EK(I)*P(I))
4       CONTINUE
        DEN=E*C-D*D
        A=((E*G-D*H)/(DEN))
        B=((C*H-D*G)/(DEN))
C THE CONSTANTS A AND B ARE KNOWN
C NOW FIND RESIDUE
        SUMM=0.
        DO 5 I=1,N
        WN(I)=(A+B*P(I))-EK(I)
5       SUMM=SUMM+W(I)*WN(I)*WN(I)
        RES=SUMM
        RETURN
        END
```

```
 EX UNIAX.FOR
FORTRAN: UNIAX
MAIN.
LIN
LINK:   Loading
[LNKXCT UNIAX Execution]

ENTER DATA FILE NO.
34

X(I),F(I),W(I) FORI= 1  .755000E+01  .625000E-01  .100000E+01
X(I),F(I),W(I) FORI= 2  .855000E+01  .125000E+00  .100000E+01
X(I),F(I),W(I) FORI= 3  .109100E+02  .137500E+00  .100000E+01
X(I),F(I),W(I) FORI= 4  .116000E+02  .250000E+00  .100000E+01
X(I),F(I),W(I) FORI= 5  .124400E+02  .312500E+00  .100000E+01
X(I),F(I),W(I) FORI= 6  .135000E+02  .375000E+00  .100000E+01
X(I),F(I),W(I) FORI= 7  .136500E+02  .437500E+00  .100000E+01
X(I),F(I),W(I) FORI= 8  .140000E+02  .500000E+00  .100000E+01
X(I),F(I),W(I) FORI= 9  .147500E+02  .562500E+00  .100000E+02
X(I),F(I),W(I) FORI=10  .148300E+02  .625000E+00  .100000E+01
X(I),F(I),W(I) FORI=11  .159600E+02  .687500E+00  .100000E+01
X(I),F(I),W(I) FORI=12  .164100E+02  .750000E+00  .100000E+01
X(I),F(I),W(I) FORI=13  .166000E+02  .812500E+00  .100000E+01
X(I),F(I),W(I) FORI=14  .200000E+02  .875000E+00  .100000E+01
X(I),F(I),W(I) FORI=15  .215000E+02  .932500E+00  .100000E+01
 AG=-.103722E+02        BG= .377017E+01
 RESO= .682176E+00      SIGU= .000000E+00      SIGO= .000000E+00
 AG=-.103722E+02        BG= .377017E+01
 RESO= .682176E+00      SIGU= .447035E-07      SIGO= .000000E+00
 AG=-.103722E+02        BG= .377017E+01
 RESO= .682176E+00      SIGU= .558794E-07      SIGO= .447035E-07
 AG=-.103460E+02        BG= .376275E+01
 RESO= .682174E+00      SIGU= .239185E-01      SIGO= .558794E-07
 AG=-.103460E+02        BG= .376275E+01
 RESO= .682174E+00      SIGU= .239185E-01      SIGO= .239185E-01
 AG=-.103440E+02        BG= .376217E+01
 RESO= .682173E+00      SIGU= .258319E-01      SIGO= .239185E-01
 AG=-.103436E+02        BG= .376207E+01
 RESO= .682173E+00      SIGU= .261189E-01      SIGO= .258319E-01

                    WEIBUL PARAMETERS ARE

 EC= .321973E-04     EM=    3.76     SIGU= .261189E-01     SIGO= 0.15634E+02

PCAL,F(I),W(I)= .618403E-01  .625000E-01  .100000E+01
PCAL,F(I),W(I)= .970441E-01  .125000E+00  .100000E+01
PCAL,F(I),W(I)= .225875E+00  .137500E+00  .100000E+01
PCAL,F(I),W(I)= .275760E+00  .250000E+00  .100000E+01
PCAL,F(I),W(I)= .342910E+00  .312500E+00  .100000E+01
PCAL,F(I),W(I)= .435352E+00  .375000E+00  .100000E+01
PCAL,F(I),W(I)= .448912E+00  .437500E+00  .100000E+01
PCAL,F(I),W(I)= .480830E+00  .500000E+00  .100000E+01
PCAL,F(I),W(I)= .549775E+00  .562500E+00  .100000E+02
PCAL,F(I),W(I)= .557114E+00  .625000E+00  .100000E+01
PCAL,F(I),W(I)= .658394E+00  .687500E+00  .100000E+01
PCAL,F(I),W(I)= .696612E+00  .750000E+00  .100000E+01
PCAL,F(I),W(I)= .712237E+00  .812500E+00  .100000E+01
PCAL,F(I),W(I)= .919005E+00  .875000E+00  .100000E+01
PCAL,F(I),W(I)= .963132E+00  .932500E+00  .100000E+01
STOP

END OF EXECUTION
CPU TIME: 1.69  ELAPSED TIME: 2:13.53
EXIT
```

BENDIN.FOR

```
C THIS PROGRAM IS FOR THE 4-POINT LOADING PURE BENDING STRESS
C PROGRAM WEIBUL THREE PARAMETERS
C THE PARAMETERS ARE SIGMAO, M ,AND C
C THIS PROGRAM COMPUTES ALL PARAMETERS BY
C LINEAR REGRESSION METHOD. FOR NOTATION SIGMAO=SIGO
C THIS PROGRAM HAS BEEN EXECUTED ON DEC-1060 SYSTEM
        DIMENSION X(20),F(20),W(20),EK(20),P(20),WN(20),WM(20)
        WRITE(5,10)
10      FORMAT(1X,'ENTER DATA FILE NO.')
        READ(5,*) ND
        READ(ND,*) N
C ND=NUMBER OF DATA FILE
C N=NUMBER OF WEIBUL POINT PAIRS
C W=ARBITRARY WEIGHTS
C X=FRACTURE STRESS VALUES
        READ(ND,*)  ((X(I),F(I),W(I)),I=1,N)
        DO 1 I=1,N
1       WRITE(5,20) (I,X(I),F(I),W(I))
20      FORMAT(1X,'X(I),F(I),W(I) FORI=',I2,3(1X,E12.6))
        DO 2 I=1,N
        EK(I)=ALOG(ALOG(1./(1.-F(I))))+ALOG(X(I))
2       CONTINUE
C V IS THE VOLUME OF TEST SPECIMEN
        V=1.0           !SHOULD BE CHANGED AS PER VOLUME
        NN=5
        JK=0
        INT=10
        RESO=1.E+30
        BEG=-.99*X(1)
        EMD=.99*X(1)
98      H=(EMD-BEG)/FLOAT(INT)
        DO 95 I=0,INT
        SIK=BEG+FLOAT(I)*H
        DO 96 II=1,N
96      P(II)=ALOG(X(II)-SIK)
        CALL LIN(W,WN,P,EK,N,SIK,A,B,RES)
        IF(RES.GT.RESO) GO TO 95
        RESO=RES
        SIG=SIK
        AG=A
        BG=B
        J=I
95      CONTINUE
        WRITE(5,80) AG,BG,RESO,SIG,SIGO
C REDIFINE EMD AND BEG AND CONTINUE
        IF (JK.GT.NN) GO TO 97
        JK=JK+1
        IF (J.EQ.0) J=1
        IF (J.EQ.INT) J=INT-1
        EMD=BEG+FLOAT(J+1)*H
        BEG=EMD-2.*H
        RESO=RES
```

```
      SIGO=SIG
      GO TO 98
80    FORMAT(2X,°AG=°,E12.6,7X,°BG=°,E12.6/,2X,°RESO=°,E12.6,
    1 5X,°SIG=°,E12.6,5X,°SIGO=°,E12.6)
C EC,ESIGO, AND EM ARE THREE WEIBULL PARAMETERS
97    SIGG=-((AG-ALOG(V/2)+ALOG(BG))/(BG-1.))
      SIGO=EXP(SIGG)
      ESIGO=SIG
      EM=BG-1.
      WRITE(5,100)SIGO,EM,SIG
100   FORMAT(/,2X,°WEIBULL PARAMETERS ARE:°,/,2X,°SIGMAO=°,E12.6,
    1 5X,°m=°,E12.5,5X,°SIGU=°,E12.6/)
C CALCULATED PROBABILITIES ARE LISTED AS BELOW
      DO 130 II=1,N
130   P(II)=ALOG(X(II)-SIG)
      CALL LIN(W,WM,P,EK,N,SIG,A,B,RES)
      DO 108 I=1,N
      PCAL=1.0-EXP(-(V/(2*(EM+1.)))*(1.-(ESIGO/X(I)))
    1 *((X(I)-ESIGO)/SIGO)**EM)
108   WRITE(5,110) PCAL,F(I),W(I),WM(I)
110   FORMAT(1X,°PCAL,F(I),W(I),WM(I)=°,E12.6,3(1X,E12.6))
      STOP
      END
C SUBROUTINE LIN CALCULATES VALUES OF CONSTANTS A AND B WHICH
C REPRESENTS A STRAIGHT LINE Y=A+BX
      SUBROUTINE LIN(W,WN,P,EK,N,SIG,A,B,RES)
      DIMENSION  W(20),P(20),EK(20),WN(20)
      C=0.
      D=0.
      E=0.
      G=0.
      H=0.
      DO 4 I=1,N
      C=C+(W(I))
      D=D+(W(I)*P(I))
      E=E+(W(I)*P(I)*P(I))
      G=G+(W(I)*EK(I))
      H=H+(W(I)*EK(I)*P(I))
4     CONTINUE
      DEN=E*C-D*D
      A=((E*G-D*H)/(DEN))
      B=((C*H-D*G)/(DEN))
C THE CONSTANTS A AND B ARE KNOWN
C NOW FIND RESIDUE
      SUMM=0.
      DO 5 I=1,N
      WN(I)=(A+B*P(I))-EK(I)
5     SUMM=SUMM+W(I)*WN(I)*WN(I)
      RES=SUMM
      RETURN
      END
```

```
 EX BENDIN.FOR
FORTRAN: BENDIN
MAIN.
LIN
LINK:   Loading
[LNKXCT BENDIN Execution]

ENTER DATA FILE NO.
39

X(I),F(I),W(I) FORI= 1  .100000E+02  .300580E+00  .100000E+01
X(I),F(I),W(I) FORI= 2  .120000E+02  .469116E+00  .100000E+01
X(I),F(I),W(I) FORI= 3  .150000E+02  .699000E+00  .100000E+01
X(I),F(I),W(I) FORI= 4  .170000E+02  .814079E+00  .100000E+01
X(I),F(I),W(I) FORI= 5  .200000E+02  .922720E+00  .100000E+01
 AG=-.555965E+01        BG= .328826E+01
 RESO= .540424E-03      SIG= .198000E+01     SIGO= .000000E+00
 AG=-.440115E+01        BG= .295214E+01
 RESO= .182929E-04      SIG= .316800E+01     SIGO= .198000E+01
 AG=-.455440E+01        BG= .299725E+01
 RESO= .614190E-07      SIG= .300960E+01     SIGO= .316800E+01
 AG=-.456974E+01        BG= .300175E+01
 RESO= .321890E-07      SIG= .299376E+01     SIGO= .300960E+01
 AG=-.456360E+01        BG= .299995E+01
 RESO= .604957E-08      SIG= .300010E+01     SIGO= .299376E+01
 AG=-.456360E+01        BG= .299995E+01
 RESO= .604957E-08      SIG= .300010E+01     SIGO= .300010E+01
 AG=-.456348E+01        BG= .299991E+01
 RESO= .602020E-08      SIG= .300022E+01     SIGO= .300010E+01

 WEIBULL PARAMETERS ARE:
 SIGMAO= .399856E+01      m= 0.19999E+01     SIGU= .300022E+01

PCAL,F(I),W(I),WM(I)= .300582E+00  .300580E+00  .100000E+01  .891089E-05
PCAL,F(I),W(I),WM(I)= .469106E+00  .469116E+00  .100000E+01 -.289977E-04
PCAL,F(I),W(I),WM(I)= .699021E+00  .699000E+00  .100000E+01  .574887E-04
PCAL,F(I),W(I),WM(I)= .814066E+00  .814079E+00  .100000E+01 -.416636E-04
PCAL,F(I),W(I),WM(I)= .922722E+00  .922720E+00  .100000E+01  .768900E-05
STOP

END OF EXECUTION
CPU TIME: 0.94  ELAPSED TIME: 1:5.62
EXIT
```

HOLLOW.FOR


```
      PROGRAM BENDIN
C* THIS PROGRAM IS FOR 4-POINT BENDING HOLLOW CERAMIC ROD
      REAL L,M(40)
      DIMENSION EPF(40),TPF(40),W(40),AA(5),P(40)
      COMMON /PAR/I,L,C,M,EI,SIGU,EM,RO,RI
      WRITE(5,40)
40    FORMAT(2X,'ENTER DATA FILE NOUMBER AND ERROR BOUND')
      READ(5,*)ND,ERR
C* K=NO. OF DATA POINTS
C* P=LOAD VALUES
      READ(ND,*) L,RO,RI
      READ(ND,*)K
      KS=1
      READ(ND,*) P(1),W(1)
      DO 22 I=2,K
      READ(ND,*) P(I),W(I)
      IF (P(I).EQ.P(I-1)) GO TO 22
      KS=KS+1
22    CONTINUE
      X=FLOAT(KS+1)
C* NOW DO RANK METHOD
      J=1
      EPF(1)=1./X
      DO 1 I=2,K
      EPF(I)=EPF(I-1)
      IF (P(I).EQ.P(I-1)) GO TO 1
      J=J+1
      EPF(I)=FLOAT(J)/X
1     CONTINUE
      WRITE(5,21) ((J,EPF(J)),J=1,K)
21    FORMAT(1X,'J=',I2,'EPF(J)=',F7.5)
      WRITE(5,41)
41    FORMAT(1X,'ENTER L,RO,RI,ERR')
C* NOW CALCULATE MOMENT FROM LOAD VALUES
      DO 2 I=1,K
2     M(I)=P(I)*3.5/2.
      EI=(3.14/4.)*(RO**4-RI**4)
      WRITE(5,59)L,RO,RI,ERR,EI
59    FORMAT(/,3X,'L=',1X,F7.3,3X,'RO=',1X,F6.3,3X,'RI=',1X,
     1 F6.3,3X,'ERR=',1X,F7.5,3X,'EI=',1X,F7.4,/)
C* NN=CODE NO. (EITHER 1 OR 2 OR 3)
C* L=GAGE LENGTH OF SPECIMEN
C* FOR NN=1  (C VARIES) ** NN=2 (EM VARIES) ** NN=3 (SIGU VARIES)
11    WRITE(5,42)
42    FORMAT(1X,'INPUT C,EM,SIGU,NN(CODE),FINAL,NOS')
      READ(5,*)C,EM,SIGU,NN,FINAL,NOS
      AA(1)=C
      AA(2)=EM
      AA(3)=SIGU
      IF(NOS.EQ.0) GO TO 58
      IF(NN.EQ.[illegible].)GO TO 59
      [illegible]=(FINAL-AA(NN))/FLOAT(NOS)
5[illegible]  II=NOS+1
      DO 10 IJ=1,II
```

```
      DO 17 I=1,K
      VAR=AA(NN)+FLOAT(IJ-1)*ENC
      N=4
      IF (NN.EQ.1) C=VAR
      IF (NN.EQ.2) EM=VAR
      IF (NN.EQ.3) SICU=VAR
      CALL ACAR(EPR,N,BN,XX)
      TPF(I)=XX
17    CONTINUE
C* NOW COMPUTE RESIDUES
      RES=0.
      DO 5 I=1,K
      WN=(EPF(I)-TPF(I))
5     RES=RES+W(I)*WN*WN
      IF(NN.EQ.1)WRITE(5,15)VAR,EM,SICU,RES
      IF(NN.EQ.2)WRITE(5,16)C,VAR,SICU,RES
      IF(NN.EQ.3)WRITE(5,18)C,EM,VAR,RES
15    FORMAT(1X,°VAR:C=°,E14.6,2X,°EM=°,1X,F6.3,2X,°SICU=°,
     1 1X,E10.3,2X,°RES=°,1X,E14.6)
16    FORMAT(1X,°C=°,1X,E13.7,1X,°VAR:EM=°,1X,F8.3,1X,°SICU=°,
     1 1X,E10.3,1X,°RES=°,1X,E14.6)
18    FORMAT(1X,°C=°,1X,E12.7,1X,°EM=°,1X,F6.3,1X,°VAR:SICU=°,1X,
     1 E14.6,1X,°RES=°,1X,E14.6)
      IF(NOS.NE.0) GO TO 10
      DO 81 I=1,K
      WRITE(5,79) (I,EPF(I),TPF(I),W(I))
79    FORMAT(1X,°EPF(I),TPF(I),W(I) FOR I=°,I2,3(2X,E13.5))
81    CONTINUE
10    CONTINUE
      GO TO 11
89    STOP
      END
```

```
      SUBROUTINE ACAR(ERR,N,BN,XXX)
      REAL L,M(40)
      COMMON /PAR/ I,L,C,M,EI,SICU,EM,RO,RI
C* SIMPSON RULE PROGRAM FOR CIRCULAR BENDINC CASE
C* A AND B ARE LOWER AND UPPER LIMIT OF INTECRATION
C* FOR FIRST PART OF INTECRATION
C* D AND A ARE LOWER AND UPPER LIMIT OF INTTECRATION FOR
C* SECOND PART OF INTEGRATION
C* N IS THE NUMBER OF SUBDIVISION
C* DX IS THE INTERVAL
C* C,EM,AND SICU ARE MATERIAL PARAMETERS
      FN=FLOAT(N)
      BNT=0.
C* EI=MOMENT OF INERTIA
C* M=BENDINC MOMENT
C* D IS Y-THRESHOLD
C* THREE CASES HAVE BEEN CONSIDERED FOR Y-THRESHOLD
      A=RI
      B=RO
      D=SICU*EI/M(I)
C* CASE-1. Y-THRESHOLD CAN OCCUR OUTSIDE RO.(IF OCCURS,THEN,BN=0)
C* CASE-2. Y-THRESHOLD CAN OCCUR BETWEEN 0.AND RI
C* CASE-3. Y-THRESHOLD CAN OCCUR BETWEEN RI AND RO
100   IF(D.GE.0.AND.D.LT.A)CALL SIMP(A,B,D,FN,BN)
      IF(D.GT.A.AND.D.LT.B)CALL SIMM(A,B,D,FN,BN)
      IF(D.GT.B) GO TO 3
C* XXX=THEROTICAL PROBABILITY OF FRACTURE
      XXX=1.-EXP(-BN)
      IF(ABS(BN-BNT).LE.ERR) RETURN
      BNT=BN
      FN=FN*2
      GO TO 100
3     BN=0.
      XXX=0.
      RETURN
      END
      SUBROUTINE SIMP(A,B,D,FN,BN)
      REAL NN
      REAL L,M(40)
      COMMON /PAR/ I,L,C,M,EI,SICU,EM,RO,RI
      II=IFIX(FN)
      DX1=(B-A)/FN
      DX2=(A-D)/FN
      TDX1=2.*DX1
      TDX2=2.*DX2
      EN11=CRANF1(A)+GRANF1(B)
      EN12=CRANF2(D)+CRANF2(A)
C NOW INITIALISE EN2 AND EN3
      EN21=0.
      EN22=0.
      EN31=0.
      EN32=0.
      NN=FN/2.
      DO 5 J=1,II-1,2
      Y1=A+DX1*FLOAT(J)
      Y2=D+DX2*FLOAT(J)
      EN21=EN21+CRANF1(Y1)
      EN22=EN22+CRANF2(Y2)
```

```
5       CONTINUE
        Y1=A
        Y2=D
        NM=IFIX(NN)-1
        DO 4 J=1,NM
        Y1=Y1+TDX1
        Y2=Y2+TDX2
        EN31=EN31+GRANF1(Y1)
4       EN32=EN32+GRANF2(Y2)
        BN=(DX1*(EN11+4.*EN21+2.*EN31)/3.)+(DX2*(EN12+4.*EN22
     1  +2.*EN32)/3.)
        RETURN
        END
        FUNCTION GRANF1(Y)
        REAL L,M(40)
        COMMON /PAR/ I,L,C,M,EI,SICU,EM,RO,RI
        SIG=M(I)*Y/EI
        IF((SIG-SICU).LT.0)SIG=SICU
060     FORMAT(2X,'M,Y,SICU,SIG,(WHEN SIG-SICU.LT.0)=',1X,4F10.4)
        GRANF1=(2.*L*C)*(((M(I)*Y/EI)-SICU)**EM)*
     1  ((RO*RO-Y*Y)**.5)
        RETURN
        END
        FUNCTION GRANF2(Y)
        REAL L,M(40)
        COMMON /PAR/ I,L,C,M,EI,SICU,EM,RO,RI
        SIG=M(I)*Y/EI
        IF((SIG-SICU).LT.0)SIG=SICU
070     FORMAT(2X,'M,Y,SICU,SIG,(WHEN SIG-SICU.LT.0 IN GF2)=',4E10.4)
        GRANF2=(2*L*C)*(((M(I)*Y/EI)-SICU)**EM)*
     1  (((RO*RO-Y*Y)**.5)-((RI*RI-Y*Y)**.5))
        RETURN
        END
        SUBROUTINE SIMM(A,B,D,FN,BN)
        REAL NN
        II=IFIX(FN)
        DX1=(B-D)/FN
        TDX1=2.*DX1
        EN11=GRANF1(D)+GRANF1(B)
C** NOW INITIALISE EN2 AND EN3
        EN21=0.
        EN31=0.
        NN=FN/2.
        DO 5 J=1,II-1,2
        Y1=D+DX1*FLOAT(J)
        EN21=EN21+GRANF1(Y1)
5       CONTINUE
        Y1=D
        NM=IFIX(NN)-1
        DO 4 J=1,NM
        Y1=Y1+TDX1
4       EN31=EN31+GRANF1(Y1)
        BN=(DX1*(EN11+4.*EN21+2.*EN31)/3.)
        RETURN
        END
```

NEWTON.FOR

```
      PROGRAM NEWTON
C* NEWTON-RAPHSON METHOD
C* PROGRAM WEIBUL THREE PARAMETERS
C* THE PARAMETERS ARE C, M, AND SIGU
C* THIS PROGRAM COMPUTES ALL PARAMETERS BY
C* NEWTON-RAPHSON METHOD
      DIMENSION X(20),F(20),W(20),A(20,20),Z(20),B(20)
      DIMENSION U(20),UIJ(20,3),U1(20),U3(20),UIKJ(20,3,3)
      WRITE(5,10)
10    FORMAT(1X,°ENTER DATA FILE NO.°)
      READ(5,*)ND
      READ(ND,*)N
C* ND=NO. OF DATA FILE
C* N= NO. OF WEIBUL POINT PAIRS
C* W= ARBITRARY WEIGHTS ASSIGNED TO DATA POINTS
C* X= FRACTURE STRESS VALUES
      READ(ND,*)((X(I),F(I),W(I)),I=1,N)
      DO 1 I=1,N
1     WRITE(5,20)(I,X(I),F(I),W(I))
20    FORMAT(1X,°X(I),F(I),W(I) FORI=°,I2,3(1X,E12.6))
C* NOW SET THE VARIOUS SUMMATIONS FOR THE LEAST SQUARE
C* METHOD, BUT FIRST MAKE A GUESS FOR C, SIGU, AND M
12    WRITE(5,24)
24    FORMAT(1X,°INPUT THE GUESSES FOR C,SIGU,EM°)
      READ(5,*)C,SIGU,EM
11    DO 3 I=1,N
      T=(X(I)-SIGU)
      IF(T.LT.0.) T=0.
      U(I)=C*T**EM
      S1=EXP(-U(I))
      S2=S1*S1
      U1(I)=W(I)*((1.-F(I))*S1-S2)
      U3(I)=W(I)*(2.*S2-(1.-F(I))*S1)
      UIJ(I,1)=U(I)/C
      UIJ(I,2)=-U(I)*EM/T
      UIJ(I,3)=U(I)*ALOG(T)
      UIKJ(I,1,1)=0.
      UIKJ(I,1,2)=UIJ(I,2)/C
      UIKJ(I,2,1)=UIKJ(I,1,2)
      UIKJ(I,2,2)=-(EM-1.)*UIJ(I,2)/T
      UIKJ(I,1,3)=UIJ(I,3)/C
      UIKJ(I,3,1)=UIKJ(I,1,3)
      UIKJ(I,2,3)=(1.+EM*ALOG(T))*UIJ(I,2)/EM
      UIKJ(I,3,2)=UIKJ(I,2,3)
      UIKJ(I,3,3)=U(I)*(ALOG(T))**2
3     CONTINUE
C* NOW FORM THE MATRIX B(I), AND A(I,J)
C* ZERO OUT A AND B
      DO 30 I=1,3
      B(I)=0.
      DO 30 J=1,3
      A(I,J)=0.
```

```
30      CONTINUE
        DO 4 I=1,N
        DO 4 J=1,3
        B(J)=B(J)+U1(I)*UIJ(I,J)
        DO 4 K=1,3
        A(J,K)=A(J,K)+U1(I)*UIKJ(I,K,J)+U3(I)*UIJ(I,J)*UIJ(I,K)
4       CONTINUE
        CALL SOLVE(A,Z,B,3,DET,5)
        WRITE(5,13)(Z(I),I=1,3)
13      FORMAT(1X,°DC,DSIGU,DM=°,E15.6)
        C=C-Z(1
        SIGU=SIGU-Z(2)
        EM=EM-Z(3)
        WRITE(5,14)C,SIGU,EM
14      FORMAT(1X,°NEW WEIBULL PARAMETERS ARE: C,SIGU,EM=°,3E15.6)
        ITES1=1HY
        WRITE(5,15)
15      FORMAT(1X,°DO YOU WISH TO CONTINUE WITH PRESENT CORRECTIONS°,
     1  /,°ANSWER Y OR N°)
        READ(5,16)ITE
16      FORMAT(A1)
        IF(ITE.EQ.ITES1) GO TO 11
        WRITE(5,17)
17      FORMAT(1X,°DO YOU WANT TO STOP-ANSWER Y OR N°)
        READ(5,16)ITE
        IF(ITE.EQ.ITES1)GO  TO 21
        GO TO 12
21      WRITE(5,100)C,EM,SIGU
100     FORMAT(/,2X,°C=°,E12.6,5X,°EM=°,E12.6,5X,°SIGU=°,E12.6/)
        STOP
        END
        SUBROUTINE SOLVE(A,X,B,N,DET,NP)
        DIMENSION B(20),X(20),A(20,20),K(20),Y(20)
         DO 16 I=1,N
   16    K(I)=I
         N1=N-1
      DET=1.
      SIG=1.
         DO 8 L=1,N1
C ****   SEARCH FOR LARGEST ELEMENT
C       NP=UNIT NUMBER OF PRINTER
         D=0.
         DO 1 L1=L,N
         DO 1 L2=L,N
         IF(ABS(A(L1,L2))-ABS(D)) 1,1,1550
 1550    D=A(L1,L2)
         ID=L1
         JD=L2
    1    CONTINUE
         IF(D)2,99,2
C **** INTERCHANGE ROWS AND COLUMNS TO PUT LARGEST ELEMENT ON DIAGONAL
    2 IF (JD.EQ.L) GO TO 14
```

```
      SIG=-SIG
      IEMP=K(L)
      K(L)=K(JD)
      K(JD)=IEMP
      DO 4 I=1,N
      TEMP=A(I,L)
      A(I,L)=A(I,JD)
    4 A(I,JD)=TEMP
   14 IF (ID.EQ.L) GO TO 15
      SIG=-SIG
      DO 3 J=L,N
      TEMP=A(L,J)
      A(L,J)=A(ID,J)
    3 A(ID,J)=TEMP
      TEMP=B(L)
      B(L)=B(ID)
      B(ID)=TEMP
   15 B(L)=B(L)/D
C***ELIMINATE ELEMENTS IN COLUMN UNDER LARGEST ELEMENT
      L1=L+1
      DO 5 J=L1,N
    5 A(L,J)=A(L,J)/D
      DET=DET*D
      DO 7 I=L1,N
      IF(A(I,L)) 1515,7,1515
 1515 D1=A(I,L)
      DO 6 J=L1,N
    6 A(I,J)=A(I,J)-D1*A(L,J)
      B(I)=B(I)-D1*B(L)
    7 CONTINUE
    8 CONTINUE
      IF(A(N,N)) 9,99,9
C***BACK SUBSTITUTE TO SOLVE
    9 Y(N)=B(N)/A(N,N)
      DET=DET*A(N,N)*SIG
      DO 11 L=1,N1
      LL=N-L+1
      D1=B(LL-1)
      DO 10 J=LL,N
   10 D1=D1-A(LL-1,J)*Y(J)
   11 Y(LL-1)=D1
C**** RE-ORDER ANSWER
      DO 12 I=1,N
      J=K(I)
   12 X(J)=Y(I)
      GO TO 13
99      WRITE(NP,100)
100     FORMAT(2X,'MATRIX IS SINGULAR NO SOLUTION GIVEN')
      DET=0.
   13 RETURN
      END
```

APPENDIX F

APPENDIX F

DISTRIBUTION LIST FOR N00019-78-C-0520

	NO OF COPIES
Commander Naval Air Systems Command Washington, DC 20361 Attention: AIR-00D4 6 AIR-320A 1 AIR-5163D4 4	11
Office of Naval Research 800 N. Quincy Street Arlington, VA 22217 Attention: Code 471	1
Commander Naval Surface Weapons Center White Oak Silver Spring, MD 20910 Attention: Code R31	1
Director Naval Research Laboratory Washington, DC 20375 Attention: Code 6360	1
Commanding Officer David W. Taylor Naval Ship Research & Development Center Annapolis, MD 21412 Attention: W. Smith, Code 2832	1
Commander Air Force Wright Aeronautical Laboratories Wright-Patterson Air Force Base Dayton, OH 45433 Attention: Dr. J. Dill POSL 1 Dr. H. Graham MLLM 1	2
Brookhaven National Laboratory Upton, NY 11973 Attention: Dr. D. Van Rooyen	1
Director Applied Technology Laboratory US Army Research & Technology Laboratories Fort Eustis, VA 23604 Attention: DAVOL-ATL-ATP (Mr. Pauze)	1
US Army Research Office Box CM, Duke Station Durham, NC 27706 Attention: CRCARD	1

	NO OF COPIES
Army Materials and Mechanics Research Center Watertown, MA 02172 Attention: Dr. R. N. Katz	1
NASA Headquarters Washington, DC 20546 Attention: C. F. Bersch, RTM-6	1
NASA Lewis Research Center 21000 Brookpark Road Cleveland, OH 44135 Attention: Dr. E. Zaretsky 1 W. A. Sanders (49-1) 1 and Dr. T. Hergel 1	2
Defense Advanced Research Project Office 1400 Wilson Blvd Arlington, VA 22209 Attention: Dr. Van Reuth	1
Inorganic Materials Division Institute for Materials Research National Bureau of Standard Washington, DC 20234	1
Department of Engineering University of California Los Angeles, CA 90024 Attention: Profs. J. W. Knapp and G. Sines	1
Engineering Experiment Station Georgia Institute of Technology Atlanta, GA 30322 Attention: J. D. Walton	1
University of Illinois College of Engineering 204 Ceramics Building Urbana, IL 61801 Attention: Sherman D. Brown Department of Ceramic Engineering	1
Department of Engineering Research North Carolina State University Raleigh, NC 27607 Attention: Dr. H. Palmour	1
Ceramic Science and Engineering Section Pennsylvania State University University Park, PA 16802 Attention: Dr. R. E. Tressler	1
Rensselaer Polytechnic Institute 110 Eighth Street Troy, NY 12181 Attention: R. J. Diefendorf	1

	NO OF COPIES
School of Ceramics Rutgers, The State University New Brunswick, NJ 08903	1
Virginia Polytechnic Institute Minerals Engineering Blacksburg, VA 20460 Attention: Dr. D. P. H. Hasselman	1
Advanced Mechanical Technology Inc. 141 California Street Newton, MA 02158 Attention: Dr. Walter D. Syniuta	1
Aerospace Corporation Materials Laboratory P.O. Box 95085 Los Angeles, CA 90045	1
Batelle Memorial Institute 505 King Avenue Columbus, OH 43201 Attention: Ceramics Department 1 Metal & Ceramic Information Center 1	2
Research and Development Division Carborundum Company Niagra Falls, NY 14302 Attention: Mr. C. McMurty	1
Ceramic Finishing Company Box 498 State College, PA 16801	1
Ceradyne Inc. Box 1103 Santa Ana, CA 92705	1
Coors Porcelain Company 600 Ninth Street Golden, CO 80401 Attention: Research Department	1
Federal-Mogul Corporation Anti-Friction Bearing R&D Center 3980 Research Park Drive Ann Arbor, MI 48104 Attention: D. Glover	1
Metallurgy and Ceramics Research Department General Electric R&D Laboratories P.O. Box 8 Schenectady, NY 12301	1

	NO OF COPIES
Hughes Aircraft Company Culver City, CA 90230 Attention: M. N. Gardos	1
IIT Research Institute 10 West 35th Street Chicago, IL 60616 Attention: Ceramics Division	1
Kaweki-Berylco Industry Box 1462 Reading, PA 19603 Attention: Mr. R. J. Longnecker	1
Research & Development Division Arthur D. Little Company Acorn Park Cambridge, MA 02140	1
Mechanical Technology, Inc. 968 Albany-Shaker Road Latham, NY 12110 Attention: Dr. E. F. Finkin	1
Norton Company Industrial Ceramics Division One New Bond Street Worchester, MA 01606 Attention: Dr. M. Torti	1
Ceramic Division Sandia Corporation Albuquerque, NM 87101	1
SKF Technology Services SKF Industries Inc. 1100 First Street P.O. Box 515 King Of Prussia, PA 19406 Attention: P. A. Madden	1
Southwest Research Institute P. O. Drawer 28510 San Antonio, TX 78228	1
Materials Sciences & Engineering Laboratory Stanford Research Institute Menlo Park, CA 94025 Attention: Dr. Cubiciotti	1

	NO OF COPIES
Teledyne CAE 1330 Laskey Road Toledo, OH 43601 Attention: Hugh Gaylord	1
Union Carbide Corporation Parma Technical Center P. O. Box 6116 Cleveland, OH 44101	1
Materials Sciences Laboratory United Technologies East Hartford, CT 06101 Attention: Dr. J. J. Brennan	1
United Technologies Research Center East Hartford, CT 06108 Attention: F. L. Ver Snyder	1
Astronuclear Laboratory Westinghouse Electric Corporation Box 10864 Pittsburgh, PA 15236	1
Westinghouse Research Laboratories 1310 Beulah Road Churchill Borough Pittsburgh, PA 15235 Attention: Dr. R. Bratton	1